The role of histone demethylase Jmjd3 in the inflammatory response: generation and analysis of *in vivo* models

Betsabeh Khoramian Tusi

PhD Thesis

SEMM course in Molecular Medicine

Supervisor:
Gioacchino Natoli
Department of Experimental Oncology
European Institute of Oncology (IEO)
Milan, Italy

Internal co-supervisor:
Stefano Casola
The FIRC Institute of Molecular Oncology Foundation (IFOM)
Milan, Italy

External co-supervisor:
Manolis Pasparakis
Institute for Genetics
University of Cologne, Cologne, Germany

Table of Contents

LIST OF ABBREVIATIONS

TSS: Transcription Start Site

ChIP: Chromatin immunoprecipitation

Pol II: RNA polymerase II

PTMs: Posttranslational modifications

SAM: S-adenosylmethionine

MLL: Mixed lineage leukaemia

PHD: Plant Homeo Domain

RBCL: Red blood cell lysis

PEPCK: Phosphoenol pyruvate carboxy kinase

FIGURE INDEX

TABLE INDEX

ABSTRACT

Jmjd3, a JmjC family histone demethylase, is quickly induced by the transcription factor NF-kB in response to microbial stimuli. Jmjd3 erases trimethylated lysine 27 in histone H3 (H3K27me3), a histone mark associated with transcriptional repression and involved in lineage determination, differentiation and tissue homeostasis. However, the specific contribution of Jmjd3 induction and H3K27me3 demethylation to innate immunity and inflammation remains unknown. To define this role, we generated gene-targeted mice lacking histone demethylase using standard protocol to see the effect of this specific Histone demethylase depletion on all tissues and in particular in immune system to understand the biological functions of jmjd3 in inflammatory responses.. Strikingly, transcription of most Jmjd3 target genes was unaffected by its deletion, a few hundred genes including IL12b and Ccl5 showed mild to moderate mRNA changes associated with impaired transcription; however, no gene was completely dependent on Jmjd3 for induction. Importantly, most Jmjd3 target genes were not associated with detectable levels of H3K27me3, and the transcriptional effects of Jmjd3 absence in the window of time analyzed were uncoupled from measurable effects on this histone mark. Overall, these data demonstrate that Jmjd3 participates in fine-tuning the transcriptional output of LPS-activated macrophages in a manner that is largely independent of H3K27me3 demetylation.

INTRODUCTION

1. Chromatin structure: an overview

The eukaryotic genome is assembled as a nucleoprotein complex which is known as chromatin. This structural polymer consists of positively charged histone proteins in addition to DNA. Chromosomal DNA wraps around octamers of histones to form nucleosomes. A nucleosome consists of 147 bp of DNA wrapped nearly twice around the octamer containing two copies of each of core histones H2A, H2B, H3 and H4. Nucleosomes are separated by linker DNA of variable length and, at their basic organizational level, arranged as a series of "beads on a string" with ~10 nm diameter. Each core histone within the nucleosome contains a globular domain that mediates histone-histone interactions in the octamer and has a highly basic amino terminal tail approximately 30 residues in length. This tail extends from the surface of the nucleosome, and is extensively modified in living cells. Until now, more than 70 different sites and 8 types of histone posttranslational modifications (PTMs) have been reported, largely using protein sequencing approaches, mass spectrometry and antibody-based detection techniques (Berger 2007; Kouzarides 2007). The posttranslational modifications of histone tails identified so far include acetylation and methylation of lysines (K) and arginines (R), phosphorylation of serines (S) and threonines (T), ubiquitination, sumoylation and biotinylation of lysines as well as ADP ribosylation (Figure 1). These modifications are recognized by specific protein-protein modules (Yap and Zhou 2006).

2. Histone modifications

It was first noticed more than 35 years ago that histones in transcriptionally active chromatin are acetylated *in vivo*. This observation led to the hypothesis that covalent modifications of histones may have a role in determining the states of gene activity (Allfrey, Faulkner et al. 1964). As mentioned before, several histone-tail modifications have been identified.

Moreover, each lysine residue can be mono-, di- or tri-methylated, and similarly an arginine can accept one or two methyl groups, which greatly increases complexity. Many studies have shown that site-specific combinations of histone modifications correlate with different states of gene activity and with chromatin-associated biological events, such as transcription, DNA repair and replication. These observations eventually led to the idea of a 'histone code'(Strahl and Allis 2000). The histone code hypothesis suggests that each specific pattern of post-translational modifications of histones may constitute a code, which determines distinct DNA-templated programs such as different transcriptional outcomes. Although the histone code has been proposed ten years ago, it is still incompletely defined how the code is established, maintained and translated into function.

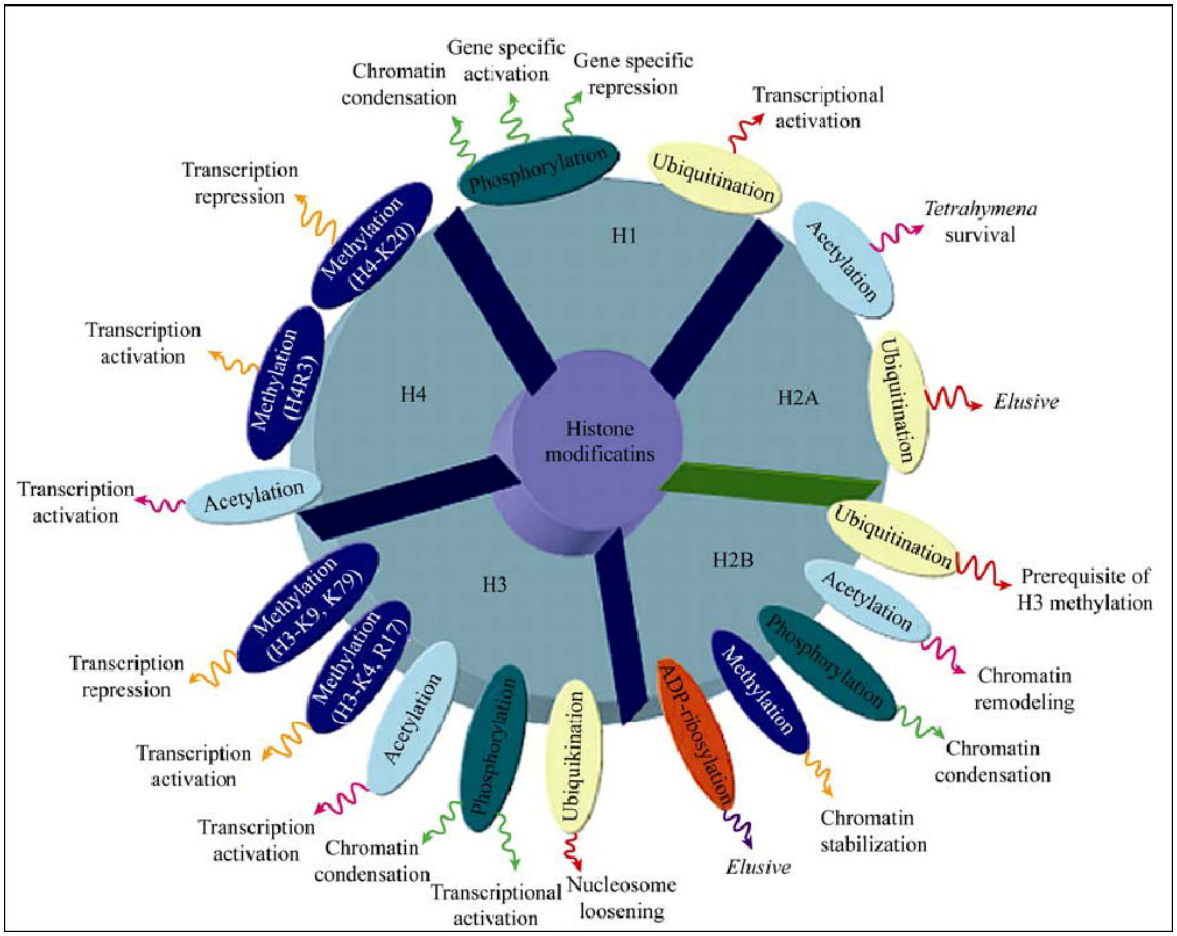

Figure 1. Schematic representation of histone modifications and their biological roles. (Munshi, Shafi et al. 2009)

The specific patterns of histone tail modifications creates local diversity, which divides the chromatin into sub-domains.

More recent findings demonstrate that certain histone modifications can actually block or facilitate additional histone modifications. This has opened up for a new concept in the field of chromatin research, which is called “Histone Crosstalk” (Suganuma and Workman 2008) . The earliest example of histone crosstalk- one histone modification promoting the generation of another - was observed on the same histone tail. That is, phosphorylation of serine 10 (S10) on histone H3 by Snf1 kinase in *Saccharomyces cerevisiae* promotes the acetylation of lysine 14 (K14) by the Gcn5 acetyltransferase on histone H3 as well. Together, these modifications increase H3’s interaction with the Bmh1 and Bmh2 proteins during gene activation (Walter, Clynes et al. 2008). Another form of crosstalk, called trans-histone crosstalk, was recently discovered by Zippo and colleagues. They showed that phosphorylation of H3 tails leads to the acetylation of H4 tails, which is required for the recruitment of the Pol II and controls the transcription of the FOSL1 gene. Basically they propose a crosstalk between modifications on two different histone tails, which determines the transcriptional outcome (Lee, Smith et al.). Nowadays, the challenge in chromatin research is not simply to identify sites of modifications but also to characterize biologically meaningful combinations of histone modification patterns and decipher “the grammar” of this complex language: what does a specific modification or combination of modifications say about the history, present function or future possibilities of the underlying DNA sequence/locus or region?

3. Histone Methylation:

Histones may be methylated on either lysine (K) or arginine (R) residues. This posttranslational modification occurs via the enzymatic addition of methyl groups from the universal methyl-group donor S-adenosylmethionine (SAM). Lysine side chains may be mono-, di- or tri-methylated, whereas the arginine side chain may be mono-methylated or di-methylated (symmetrically or asymmetrically) (Figure 2). Until now, 24 sites of methylation are known on histones (17 are lysine residues and seven are arginine residues) (Bannister and Kouzarides 2005). In mammals, histone arginine methylation is typically found on residues 2, 8, 17 and 26 of histone H3.

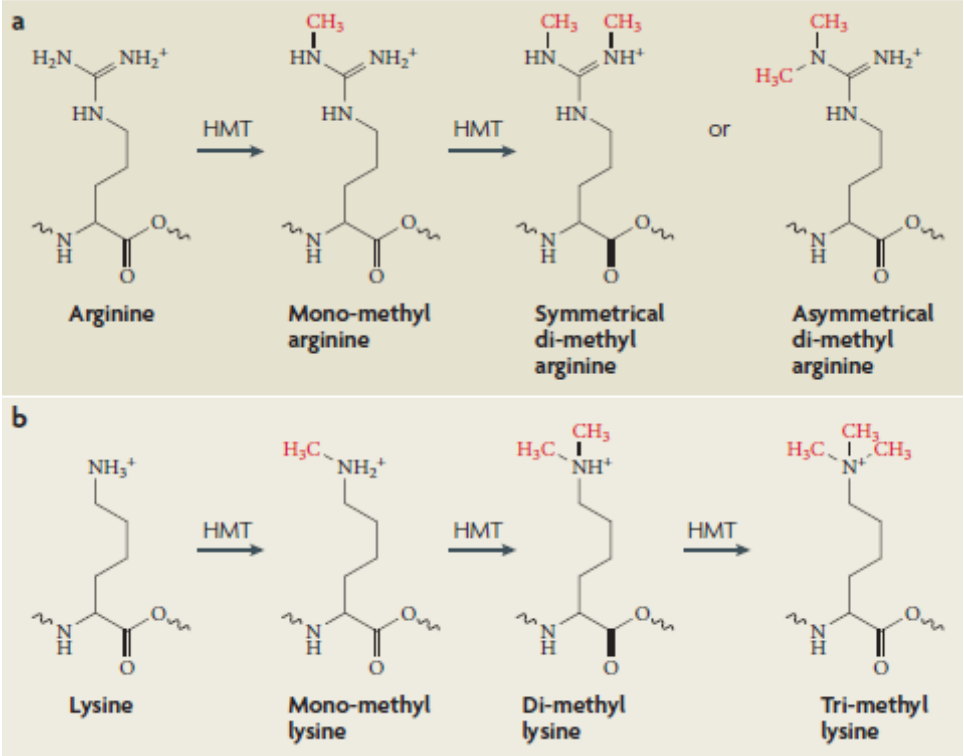

Figure 2. Methylation states of arginine and lysine residues in histones. (a) Arginine can be methylated to form mono-methyl, symmetrical or asymmetrical di-methylarginine. (b) Lysine can be methylated to form mono- di- and trimethyl lysine. Methyl groups are indicated in red. HMT, histone methyltransferase. (Klose and Zhang 2007)

It is possible that methylation induces alterations in chromatin architecture, either condensing or relaxing its structure, although it does not impact on the overall charge of the histone tail. This mark can be either a mark of actively transcribed regions or repressed chromatin, depending on the site and degree of methylation. For example, methylation of H3K4, H3K36 and H3K79 are typical of actively transcribed regions, whereas methylation of H3K9, H3K27 and H4K20 is associated with genes that are silenced or repressed (Martin and Zhang 2005). Furthermore, the methylation degree at a specific residue affects the final transcriptional outcome (Santos-Rosa, Schneider et al. 2002). Importantly, a methyl group is relatively small and its addition to lysine or arginine residues does not neutralize their charge, so it is unlikely that methylation alone will significantly affect chromatin structure but it can create binding sites for regulatory proteins that contain specialized recognition domains.

There are three classes of histone-methylating enzymes:

a) SET domain lysine methyltransferases,
b) non-SET domain lysine methyltransferases,
c) arginine methyltransferases

All three classes use S-adenosylmethionine as a co-substrate to transfer methyl groups (Smith and Denu 2009).

The SET domain-containing enzymes are the largest group among histone-methylating enzymes. SET domain proteins can be classified into five subfamilies; SET1, SET2, SUV39, RIZ (retinoblastoma protein-interacting zinc-finger) and SMYD3 (SET-and MYND-domain containing protein 3) (Table 1).

Table 1. Histone methyl transferase (HMT) classifications and specificities

Histone lysine methyl transferases	Histone substrate specificity
SET domain-containing	
SET1 family	
SET1	H3K4, H3K79
EZH2	H3K27
MLL1/4 (KMT2A/D)	H3K4
SET2 family	
SET2	H3K36
NSD1	H3K36
SUV39 family	
SUV39H1/2 (KMT1A/B)	H3K9
RIZ family	
RIZ1	H3K9
SMYD3 family	
SMYD3	H3K4
Non-SET domain-containing	
DOT1	H3K4, H3K79
Protein arginine methyl transferases	
PRMT1	H4R3
PRMT4(CARM1)	H3R2, H3R17, H3R26
PRMT5	H3R8, H4R3

Enhancer of zeste homologue 2 (EZH2) is a H3K27-specific SET1 histone methyltransferase which is associated with polycomb complexes and serves to silence homeotic genes and repress transcription (Valk-Lingbeek, Bruggeman et al. 2004).

SUV39 homologue 1 (SUV39H1) is another repressive HMT which is recruited to heterochromatic regions as well as the promoters of repressed genes (including some

controlling cell cycle), where it tri-methylates lysine 9 on histone H3, thereby recruiting the chromodomain-containing heterochromatin protein 1 (HP1) to repress transcription and delay cell cycle progression (Bannister, Zegerman et al. 2001; Lachner, O'Carroll et al. 2001). RIZ1, a H3-K9 HMT also negatively regulates proliferation and induces cell cycle arrest and apoptosis (He, Yu et al. 1998).

On the other hand, mixed lineage leukaemia (MLL), family members, SMYD3 and nuclear receptor-binding SET domain protein-1 (NSD1) activate transcription.

MLL is associated with bromodomain-containing trithorax complexes which induce chromatin decondensation (Milne, Briggs et al. 2002), and specifically mediate H3K4 methylation. SMYD3 exists in a complex with RNA polymerase II and HELZ, an RNA helicase, and is targeted to promoters containing specific DNA binding sequences where it exerts its H3-K4 methylation activity. NSD1, a SET2 subfamily member and H3-K36 HMT, is involved in developmental gene control and normal Hox gene expression (Wang, Cai et al. 2007).

4. Histone demethylation

4.1. Overview: For a long time, the methyl mark was considered as a stable histone mark because biochemical evidence indicated that the turnover of histone methyl marks was equivalent to the turnover of histones themselves; moreover, the C-N bond in the methylated histone has a thermodynamically stable nature. A number of groups proposed hypothetic mechanisms for direct histone demethylation. One possibility involved S-adenosylmethionine (SAM) as the source of a reactive radical intermediate, which would target the N-methyl group, creating an unstable aminium cation radical that would spontaneously hydrolyze to form formaldehyde and a demethylated residue (Chinenov 2002). Oxidation of the methyl group coupled to reduction of a cofactor and the release of the methyl group as formaldehyde or as another higher oxidative state, was another possibility (Bannister, Schneider et al. 2002).

Although theoretically feasible, experimental evidence was lacking for several decades until the first characterization of a histone demethylase (HDM), LSD1 [KDM1A] by Shi et al. in 2004. More recently, proteins containing the Jumonji C (JmjC) domain were demonstrated to catalyze site-specific demethylation of mono-, di-, and trimethylated histones. Overall two kinds of histone lysine demethylases have been identified, including lysine specific demethylase 1 (KDM1/LSD1) and Jumonji C (JmjC) domain family proteins.

4.2. LSD1-mediated demethylation

LSD1/KDM1, also known as KIAA0601 or BHC110, is a highly conserved protein that demethylates H3K4me1/2 but cannot attack trimethylated H3K4 (Shi, Lan et al. 2004).

4.2.1. Structure of LSD1/KDM1: The structure of LSD1 includes three domains (Fig.3)(Chen, Yang et al. 2006). It consists of a C-terminal amine oxidase-like (AOL) domain, which shows homology to flavin adenine dinucleotide (FAD)-dependent oxidases. The AOL domain includes two subdomains, a FAD-binding subdomain and a substrate-binding subdomain (Chen, Yang et al. 2006). The two subdomains form a large cavity that creates a catalytic center at their interface. The cavity is not capable of recognizing the histone substrates with different methylation states. Furthermore, LSD1 requires protonated nitrogen as the substrate for demethylation reaction, thus explaining why the trimethylated state cannot be reversed by this enzyme (Shi, Lan et al. 2004).

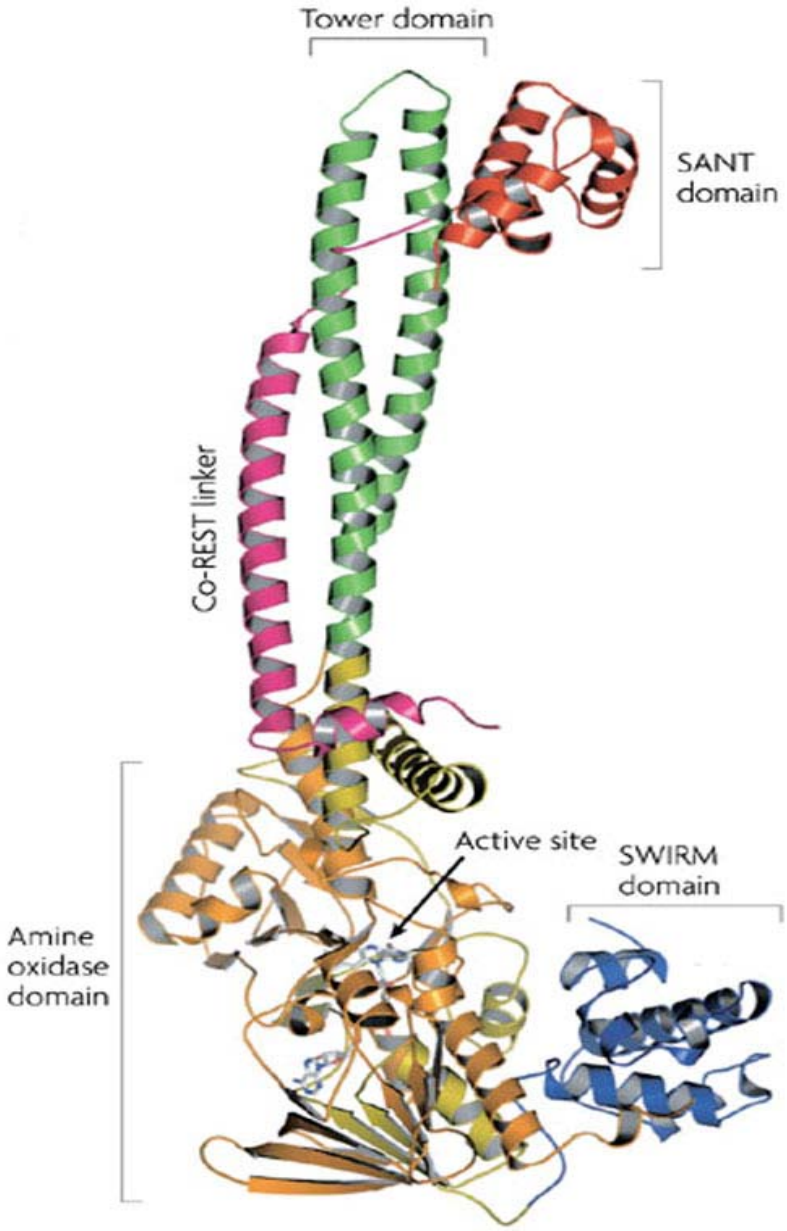

Figure 3 . Structure of LSD1 bound to Co-REST and the cofactor FAD. The two-lobed amine oxidase (AO) domain is shown in orange and yellow. The Tower domain is in green and the SWIRM domain in blue. The Co-REST linker region (pink) associates with the LSD1 Tower domain and the SANT domain (red) situated at the top of the Tower domain. (Klose and Zhang 2007)

In addition, LSD1 contains an N-terminal SWIRM domain, which is important for its stability. The SWIRM domain is bound to the AOL domain. The juxtaposition of these two domains forms a highly conserved cleft, which may serve as an additional histone tail-binding site. The third domain is the Tower domain, which is inserted into the AOL domain. The Tower domain

is important for the histone demethylase activity of LSD1. By interacting with other proteins, the Tower domain may regulate the catalytic activity of LSD1 through allosteric effects (Stavropoulos, Blobel et al. 2006).

In addition, the Tower domain directly interacts with one of the LSD1-interacting proteins, CoREST, and functions as a molecular bridge that connects LSD1 to its nucleosomal substrates (Shi, Lan et al. 2004).

4.2.2. Chemical mechanism and function of LSD1:

LSD1 is a flavin-containing amine oxidase. Basically, amine oxidase catalyzes cleavage of the α-carbon bond of the substrate to generate an imine intermediate. The intermediate is then hydrolyzed to an aldehyde and amine via a non-enzymatic process. During the whole process, the cofactor FAD is reduced to FADH and then reoxidized by oxygen to produce hydrogen peroxide (Figure 4) (Binda, Mattevi et al. 2002).

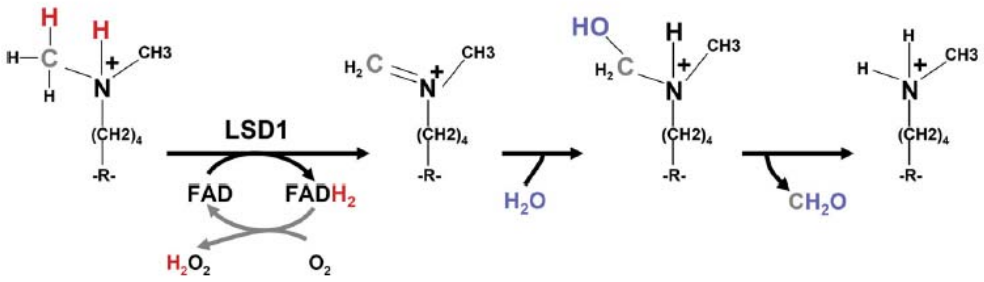

Figure 4 . Chemical Mechanism for LSD1-Mediated demethylation: In this oxidation reaction, LSD1 transfers two hydrogen atoms from methylated H3K4 to FAD to form an imine intermediate. This intermediate is then hydrolyzed to produced an unstable carbinol amine intermediate followed by a release of formaldehyde. (Shi and Whetstine 2007)

The oxidation reaction catalyzed by LSD1 depends on the cofactor FAD, and generates an unmodified lysine (H3K4) and a formaldehyde byproduct (Shi, Lan et al. 2004).

4.2.3. LSD1 associated factors:

The LSD1 complex contains other proteins, including histone deacetylases (Shi, Lan et al. 2004). LSD1 is associated with HDAC1/2, the SANT domain-containing corepressor CoREST, and the PHD domain-containing protein BHC80. HDAC and LSD1 may exist in the same complex to mediate negative regulation. It has been reported that HDAC inhibitors diminish the activity of LSD1 in *in vitro* H3K4 demethylation assays, which proved the existence of a link between the histone demethylase and deacetylase (Lee, Wynder et al. 2006). In addition, LSD1 is also a part of the transcription activation complex that includes MLL1, a H3K4 methyltransferase (Nakamura, Mori et al. 2002).

4.3. Jumonji C Domain-mediated demethylation

4.3.1. Structure and evolution of JmjC-domain-containing Proteins

The JmjC-domain-containing proteins comprise a large family that can be classified into different clusters depending on the degree of homology within the JmjC domain and on the presence of other conserved domains (Figure 5) (Takeuchi, Watanabe et al. 2006). The JmjC domain is a predicted metalloenzyme, and its catalytic motif is conserved in organisms ranging from bacteria to humans. Until now, over 100 JmjC-domain-containing enzymes have been discovered and more than 30 of them are expressed in humans (Klose, Kallin et al. 2006).

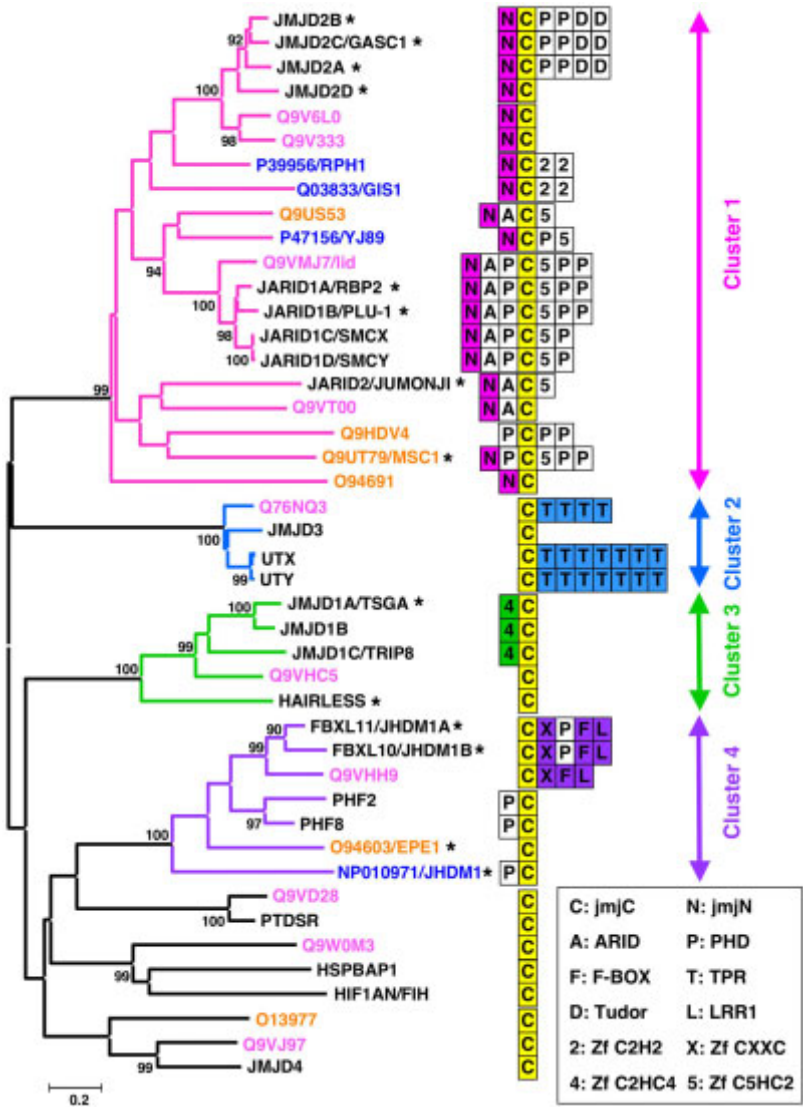

Figure 5 . JmjC-domain-containing proteins; Boxes beside protein names show domains that each protein contains. Colored boxes show characteristic domains in each cluster. Asterisks mark proteins that have been reported to be involved in gene repression or histone modification. (Takeuchi, Watanabe et al. 2006)

Currently five JmjC domain subfamilies have been characterized: JHDM1, JHDM2, JMJD2, JMJD3 and JARID1 (Tsukada, Fang et al. 2006; Whetstine, Nottke et al. 2006). The JHDM1 family represented by JHDM1A has enzymatic activity for H3K9me1 (Tsukada, Fang et al. 2006); the JHDM2 family represented by JHDM2A catalyzes H3K9me1/me2 demethylation (Yamane, Toumazou et al. 2006); the JMJD2/JHDM3 family is composed of four members, JMJD2A, B, C, D which are able to demethylate di- and trimethylated H3K9 and H3K36 (Cloos, Christensen et al. 2006; Fodor, Kubicek et al. 2006; Whetstine, Nottke et al. 2006); the

JARID family is represented by JARID1A (RBP2), JARID1B (PLU1), JARID1C (SMCX) and JARID1D which demethylate di-or tri-methylated H3K4 (Iwase, Lan et al. 2007; Yamane, Tateishi et al. 2007); the JMJD3 family includes UTX, UTY and JMJD3 which are able to demethylate di- or tri-methylated H3K27 (Agger, Cloos et al. 2007; De Santa, Totaro et al. 2007; Hong, Cho et al. 2007; Lan, Bayliss et al. 2007).

4.3.2. Chemical mechanism of JmjC-domain- mediated demethylation

JmjC-domain-containing enzymes turn over their substrates in a different manner from that of LSD1. No free electron pair on the nitrogen atom is needed, so they are able to act on trimethylated lysines as well. They need two cofactors, α-ketoglutarate and Fe^{II} ions (Trewick, McLaughlin et al. 2005) to perform the demethylation reaction (Figure 5).

During this reaction, an iron-oxo intermediate is formed. A quaternary complex consisting of the two cofactors and the substrate reacts with oxygen while bound to the active site of the enzyme. Furthermore, an electron transferred from Fe^{II} to O_2 generates a superoxide radical. This radical attacks the C_2 atom of α-ketoglutarate resulting in a bond between Fe^{IV} and α-ketoglutarate. The α-ketoglutarate is then decarboxylated, giving rise to succinate and CO_2 and the subsequent formation of a Fe^{IV}-oxo species. In the next step, the Fe^{IV}-oxo intermediate is reduced, while a hydrogen atom of the methylated substrate is removed. Again, a carbinolamine is generated, which degrades into formaldehyde and a lysine, which has one methyl group less. The Fe^{II} ion is regenerated within this step (Chen, Zang et al. 2007).

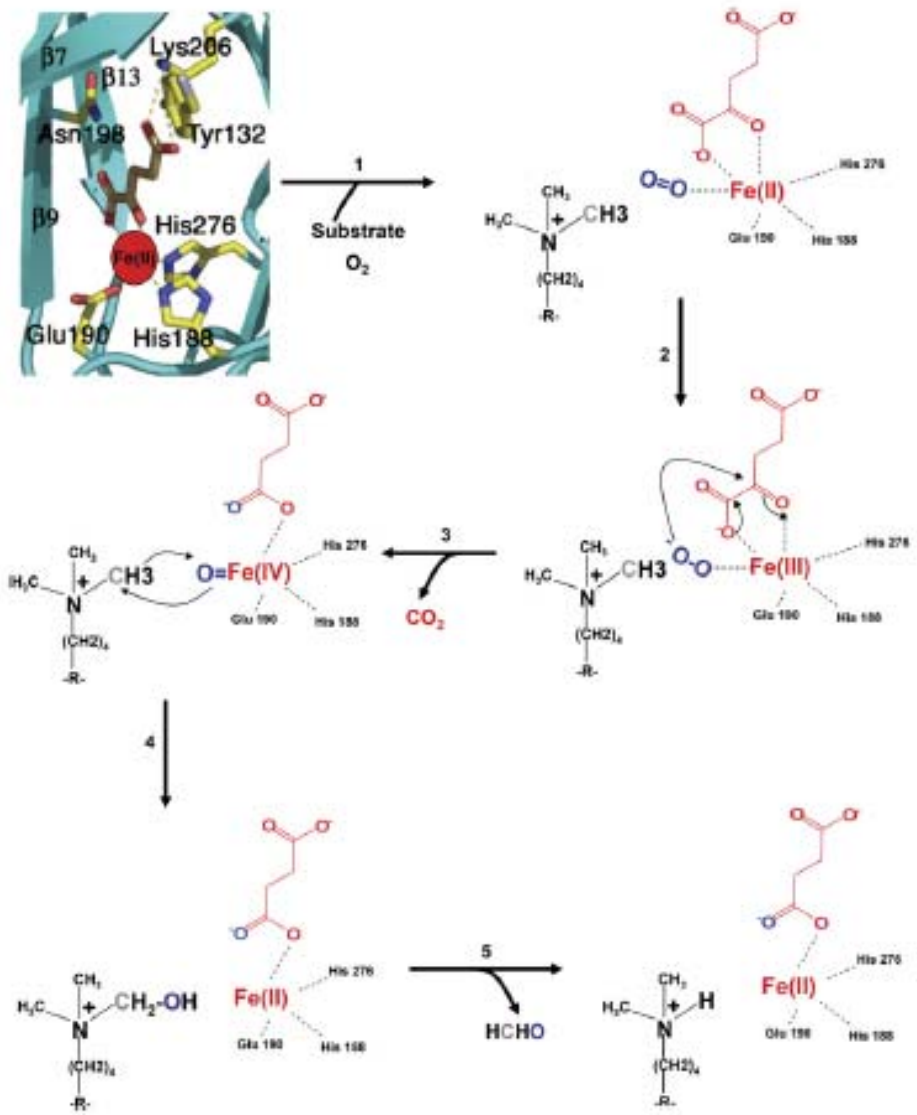

Figure 6 . Chemical Mechanism for Demethylation Mediated by the JmjC Proteins (Shi and Whetstine 2007)

To date, many of the methylated histone marks have a corresponding demethylase (Figure7).

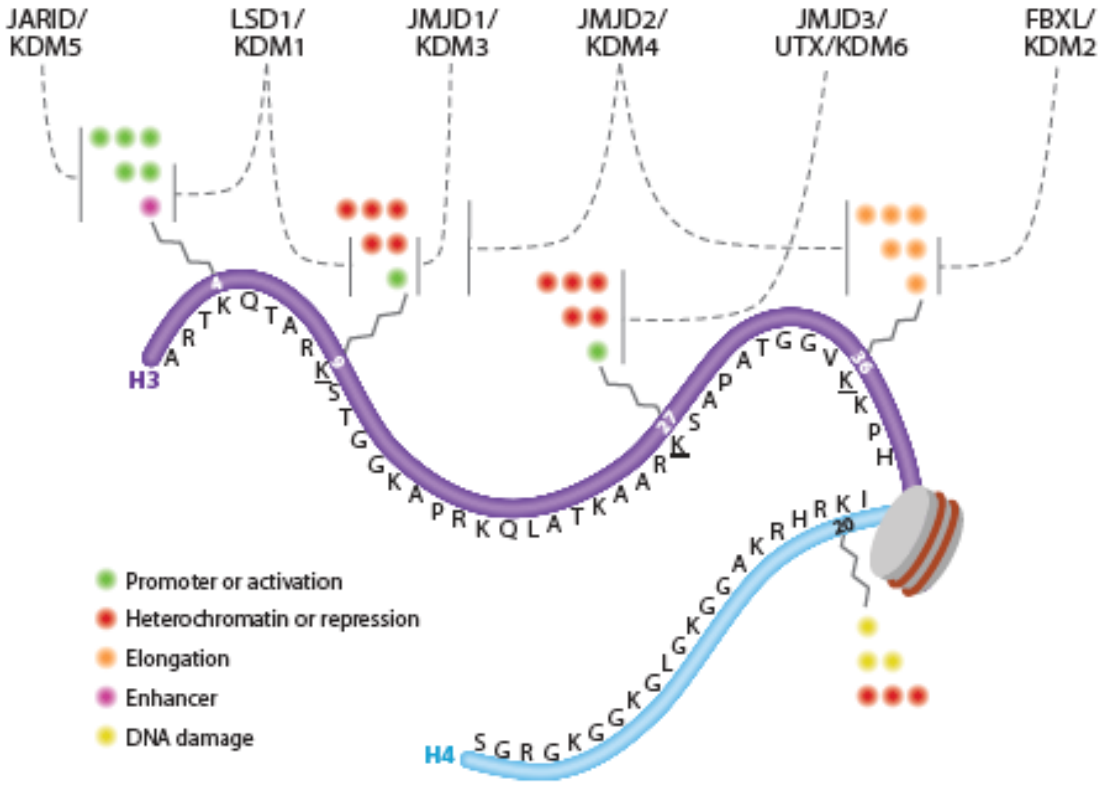

Figure 7. Substrate specificity of histone demethylases described to date. Dashed lines point to the methylated residue(s) that are demethylated by the indicated enzymes. The embedded numbers refer to the methylated amino acid residue on each histone. The general function of each mono-, di-, and trimethylation state is depicted in dots of distinct colors as shown in the figure key. Abbreviations: JARID, Jumonji and ARID domain protein (also known as KDM5); LSD1, Lysine-specific demethylase, also known as KDM1A; JMJD1, Jumonji domain protein 1, also known as KDM3; JMJD2, Jumonji domain protein 2, also known as KDM4; UTX, Ubiquitously transcribed tetratricopeptide repeat, X chromosome protein, also known as KDM6A; JMJD3, Jumonji domain protein 3, also known as KDM6B; FBXL, F-box and leucine-rich repeat Protein, also known as KDM2. (Mosammaparast and Shi 2010)

5. Methylation marks and their recognition

As mentioned, histone lysine residues can be found in monomethylated (me1), dimethylated (me2) and trimethylated (me3) states *in vivo* which is the result of the balanced enzymatic activities of histone methyltransferases and opposing demethylases (Shi and Whetstine 2007).

Genome-wide analyses show that these methylation states at particular lysine residues are enriched in certain regions of chromatin, suggesting specialized and distinct biological function. Methyl marks can be read by proteins bearing specialized recognition domains. Two general classes of protein folds that can bind methyl-lysine marks are members of the Royal superfamily (Maurer-Stroh, Dickens et al. 2003; Ruthenburg, Allis et al. 2007) and PHD fingers (Pena, Davrazou et al. 2006; Shi, Hong et al. 2006).

All methylated forms of lysine have a cationic property at physiological pH, hence trimethyl-lysine carries a positive charge. Addition of a methyl-group increases the hydrophobicity and the cation radius of the lysine methyl-ammonium group and this decreases the ability to donate hydrogen bonds concomitantly. Thus, different methylation states are diverse in the physiochemical properties of lysine, enabling state-specific readout by different effector modules.

Among the Royal superfamily members, some recognize higher lysine methylation states, K-me2 and K-me3 and some recognizes lower lysine methylation state, K-me1.

For example, chromodomains target di- and trimethyl-lysine in a H3K9 and H3K27 context. The chromodomain of HP1 interacts with H3K9me3 and the chromodomain of *D. melanogaster* Polycomb protein specifically targets H3K27me3. Although the chromodomain of HP1 and polycomb bind methylated lysines, this is not the case for all the chromodomain family members and probably the regions outside the domain are crucial in determining substrate specificity.

Another member of Royal superfamily binding to higher lysine methylation states is double chromodomains of CHD1 which targets methyl-lysine in H3K4 context. The double tudor domain of JMJD2A is another member which binds to trimethyl-lysine in a H3K4 context.

Tandom tudor domains of mammalian p53-binding protein (53BP1) binds to lower lysine methylation states. This domain targets mono- and dimethyllysine in H4K20 context. MBT repeats in human lethal-(3) malignant brain tumor repeat-like protein-1 (L3MBTL1) is another example of this group which targets mono- and dimethyllysine independently of the sequence context.

The PHD-finger family is the second group of reader modules recognizing methyl-lysine marks. This group of modules targets di- and tri-methyllysine in H3K4 context. For example, BPTF is the largest subunit of the NURF (nucleosomal remodeling factor) ATP-dependent chromatin-remodeling complex which specifically interacts through its PHD-finger domain with the H3K4me3. The PHD finger-containing human inhibitor of growth-2 (ING2) protein of the Sin3-histone deacetylase (HDAC) complex also interacts with H3K4me3 (Taverna, Li et al. 2007).

6. Histone Demethylases in Biology: key examples

The biological roles of histone demethylases strongly depends on the protein complex in which the demethylases reside. Studies on the histone demethylases in the past few years showed different roles for them in many areas of biology, ranging from cell proliferation and regulation of stem cell pluripotency to inflammatory response.

Some demethylases have a conserved role in a particular biological process. For example, LSD1(KDM1) which is a H3K4me2/1 demethylase has a particular role in meiosis in organisms ranging from yeast to mice. There is a high expression of LSD1 in the mouse testis during spermatogenesis followed by low level of H3K4me2 mark in this tissue (Godmann,

Auger et al. 2007). Mutations in fruit flies LSD1 ortholog lead to sex-specific embryonic lethality and sterility in the surviving offspring because of defects in ovary development (Di Stefano, Ji et al. 2007). Studies on *C. elegans* LSD1 ortholog also showed that mutations in this gene cause sterility and accumulation of H3K4me2 mark. This sterility was shown to correlate with disrupted gene regulation in spermatogenesis(Katz, Edwards et al. 2009).

Several histone demethylases have important role in ESC (embryonic stem cell) self-renewal. For example, JMJD1A(KDM3A) and JMJD2C(KDM4C) which demethylate H3K9me2 and H3K9me3 are activated by Oct4 in mESCs for maintaining ES cell self-renewal. These two enzymes demethylate H3K9me3/2 at the promoters of Tcl1 and Nanog and activate their transcription (Loh, Zhang et al. 2007).

Studies of human epidermis as a model for mammalian tissue self-renewal showed that JMJD3 (KDM6B), which is a H3K27me3 demethylase, may regulate the differentiation state of this tissue (Sen, Webster et al. 2008). It has also been shown that JMJD3 contributes to the activation of the INK4A-ARF locus in response to oncogene- and stress-induced senescense (Agger, Cloos et al. 2009; Barradas, Anderton et al. 2009), suggesting a tumor suppressor role for JMJD3. INK4A-ARF locus is repressed by the H3K27me3 mark (Bracken, Kleine-Kohlbrecher et al. 2007). In response to oncogenic stress, INK4A-ARF locus is activated through the removal of H3K27me3 repressive mark by upregulation of JMJD3. Some studies have been shown that JMJD3 expression is significantly decreased in several types of primary tumors, including lung and liver carcinomas and various hematopoietic malignancies (Agger, Cloos et al. 2009). Somatic mutations also found in the JMJD3-related H3K27 demethylase UTX in multiple tumors, strongly supporting a tumor suppression role for H3K27 demethylases (van Haaften, Dalgliesh et al. 2009).

Two separate studies on mouse knockout models for JHDM2A (also known as JMJD1A or KDM3A), a JmjC-Containing H3K9 demethylase have revealed a critical function of this

enzyme in animal development. This enzyme functions as a coactivator for AR (Androgen Receptor) and is required for hormone-induced H3K9 demethylation (Yamane, Toumazou et al. 2006). Hypomorphic Jhdm2a knockout model showed the important role of this enzyme in spermatogenesis and the male mice lacking this enzyme are infertile. This defect is due to the role of the demethylase in activating the expression of Tnp1 and Prm1 genes, which has a role in packaging and condensation of sperm chromatin (Okada, Scott et al. 2007). The complete knockout mice for *Jhdm2a* also showed spermatogenesis defects plus defects in metabolism which lead to obesity in this model (Tateishi, Okada et al. 2009). This study has revealed that other nuclear hormone receptors, including PPAR-γ and RXR-α are targeted by JHDM2A to promote metabolic gene activation. The mutant mice are unable to maintain proper body temperature when exposed to the cold weather showing a defect in normal metabolism in brown adipose tissue (Tateishi, Okada et al. 2009).

7. Inflammation:

Inflammation evolved as a rapid and highly beneficial response to microbial infection, tissue injury, and other insults (Smale). The inflammatory response initiates within minutes when innate immune cells, such as macrophages, encounter a microbe or another foreign or host irritant. The host cells first recognize the stimulus through a wide variety of sensing mechanisms, often involving transmembrane receptors.

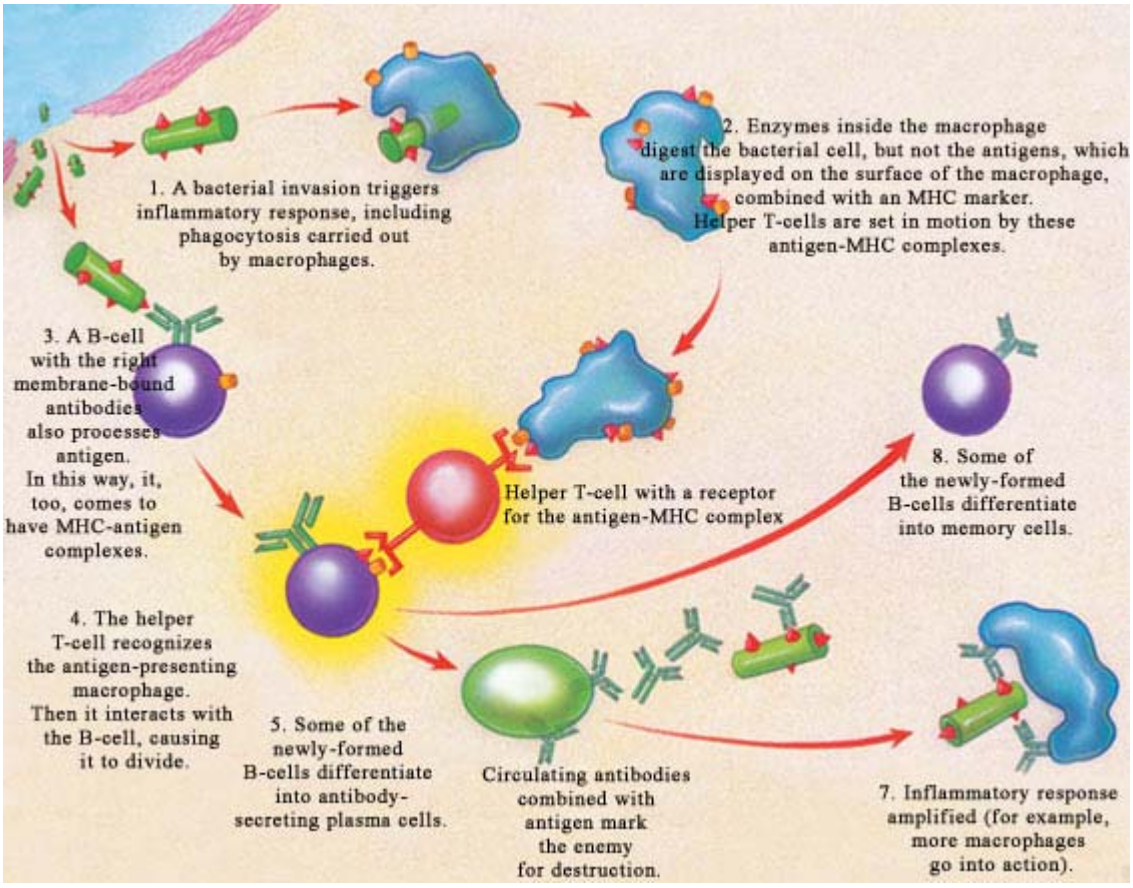

Figure 8. Schematic representation of inflammatory response

These interactions transmit signals to the nucleus, resulting in the activation of a complex gene expression program that induces the transcription of hundreds of genes over several hours or days. Some products of these inducible genes, such as antimicrobial peptides and complement factors, directly target infectious microorganisms. Others, including proinflammatory cytokines and chemokines, activate endothelial cells and recruit cells of both the innate and adaptive immune systems to the site of infection. In addition to their local effects, inducible gene products can act systemically to induce fever, the acute phase response in the liver, and other physiological changes.

There are two basic types of inflammation – acute and chronic. Acute inflammation is a short-term response, which could be anything from a few minutes to a few days.

Chronic inflammation, by contrast, is a prolonged, dysregulated and maladaptive response. It may persist for weeks, months or even years. Such persistent inflammation is associated with many chronic human conditions and diseases, including allergy, atherosclerosis, cancer, arthritis and autoimmune diseases.

8. Macrophages:

Macrophages are the major differentiated cell type of mononuclear phagocyte system and serve as key effectors in antimicrobial defense and inflammatory responses. Macrophages have many roles in development, wound healing, and homeostasis. The vital homeostatic role of macrophages involve clearing approximately 2×10^{11} erythrocytes each day which equates to almost 3 kg of iron and haemoglobin per year that is 'recycled' for the host to reuse. This clearance process is a vital metabolic contribution without which the host would not survive. They are also involved in the removal of cellular debris generating during tissue remodeling, and rapidly clear apoptotic cells. This process results in little or no production of immune mediators by unstimulated macrophages(Mosser and Edwards 2008).

As mentioned, macrophages are one of the main cell types that are recruited to the inflamed, infected tissue in the initial phase of an inflammatory response. They are known as **inflammatory cells** together with neutrophils. By nature, they exist in a benign state but are able to respond to microbial products and cytokines to mount an inflammatory response. Such stimuli arm the macrophage by activating their capacity to phagocytose, process, and present antigens. During macrophage activation, the transcriptional machinery is heavily remodelled in order to drive the changes in gene expression occurring in this context.

9. Epigenetic regulation of macrophage activation

The molecular mechanisms that regulate the expression pattern changes during macrophage activation are not fully understood.

Recent studies have been shown that epigenetic regulation via chromatin remodeling is an important event that controlled the expression pattern of specific genes. For example, in a recent study, researchers showed that M2-macrophage marker genes are epigenetically regulated by reciprocal changes in histone H3 lysine-4 (H3K4) and histone H3 lysine-27 (H3K27) methylation; and the latter methylation marks are removed by the H3K27 demethylase Jumonji domain containing 3 (Jmjd3) (Ishii, Wen et al. 2009). The induction of H3K27 demethylase Jmjd3 is dependent on STAT6 signaling pathway and the induced Jmjd3 contributes to decreasing H3K27 methylation on the promoter region of M2 marker genes and subsequent maintenance of M2 marker genes in a transcriptionally active state(Ishii, Wen et al. 2009). This study basically confirmed the role of epigenetic mechanism in gene regulation program which is happening during the activation of macrophages. Further studies need to be done to shed light on the molecular mechanism of macrophage activation.

10. Rationale of the work

Since Jmjd3 is upregulated in response to Lps stimulation (De Santa, Totaro et al. 2007), it is likely that this gene is a part of the complex gene expression program which is remodeled in response to inflammatory stimuli in order to drive changes in gene expression occurring in this context.

Our group as well as other laboratories identified the JmjC-domain proteins UTX and JMJD3 as H3K27-specific demethylases that enable the activation of genes involved in animal body patterning and the inflammatory response (Agger, Cloos et al. 2007; De Santa, Totaro et al. 2007; Lan, Bayliss et al. 2007; Lee, Villa et al. 2007). These exciting findings have broad

implications for how Polycomb-mediated silencing can be counteracted to enable changes in cell fate. However, biological implications of these findings are unavailable to date, as no animal models in vertebrates are available in which the expression of these proteins is either abrogated or increased.

Following up on these observations, the purpose of the PhD project was:

i. To define the consequences of Jmjd3 absence in
    a) Mouse development in general
    b) Inflammation in particular
ii. To define the role of Jmjd3 in normal hematopoietic development and what are the consequences of Jmjd3 deficiency on
    a) Normal hematopoiesis;
    b) Hematopoiesis in inflammation;
    c) Emergency hematopoiesis
iii. To define the whole complement of target genes regulated DIRECTLY by Jmjd3 and what are their biological function(s).
iv. How does Jmjd3 regulates activity of the genes (if any) controlled in a manner independent of H3K27me3 demethylation?

METHODS & MATERIALS

1. EMBRYO ANALYSIS:

1.1 Generation of *Jmjd3* deficient mice - To investigate the role of *Jmjd3 in vivo* we generated a constitutive knockout mouse model based on gene trap mutagenesis. Gene trapped- ESC lines are freely available through the International Gene Trap Consortium (IGTC), a public gene trap resource that can be accessed at http://www.genetrap.org/. The gene-trap cell line (XB814 BG; Gene Bank Acc: CC178692) was obtained from BayGenomics, an IGTC member laboratory in which this gene trap line had been generated by introducing the pGT0pfs gene trap vector into E14Tg2α ESCs derived from the 129/Ola strain. The pGT0pfs vector contains a splice acceptor (sA) and a promoterless lacZ-neomycin phosphotransferase fusion (βgeo) followed downstream by a polyadenylation signal (Skarnes, Moss et al. 1995; Leighton, Mitchell et al. 2001; Mitchell, Pinson et al. 2001). Its integration into an intron of a gene expressed in undifferentiated ESCs generates a fusion transcript between the upstream exon of *Jmjd3* and the βgeo construct, resulting in neomycin resistance and β-galactosidase expression.

1.1.1 Mapping the precise integration site of the gene trap vector - A PCR strategy was set up to identify the exact insertion point of the gene trap vector. The PCR was based on a reverse primer located in the trap cassette and four forward primers annealing at different sites within intron 1 of Jmjd3. A list of primers using in this PCR strategy is available below.

Primer name	Sequence (5'-3')
D35UTF1	TCTGCTGTAACCCACTGCTG
D3in1-1	GGAATGTCATGCTTCACTGCCAAG
D3in1-2	GTCTGGTGTCTTTGGTCGTCCAG
D3in1-3	GCACTTGACCACAGTTTAGCGT
bGeo-1	AGTATCGGCCTCAGGAAGATCG

1.1.2 PCR genotyping – After identification the insertion point of the trap cassette in intron one of Jmjd3, a triplex PCR-based strategy was designed to distinguish the trapped from the wild-type allele using the primers listed below.

Primer name	Sequence (5'-3')
JBaygd	AGGATACAGGAGCCACGCG
JBaygr	TGACTCTCCACTCGATCACCC
GTrev	TCCGGAGCGGATCTCAAAC

The confirmed clone was used for blastocyst injection and generation of chimeric mice. In spite of the low-level chimerism, germline transmitted mice were obtained. Heterozygous Jmjd3$^{+/-}$ mice were bred with each other to generate homozygouse knockout animals.

1.2 Histological Analyses - Whole body histological analyses performed on the E18.5 embryos fixed in 4% paraformaldehyde-1-phosphate-buffered saline (PBS). For this purpose, the samples were sent to the pathology core of CMHD (The Centre for Modeling Human Disease) in Toronto, Canada.

2. MAMMALIAN CELL CULTURE

2.1 Foetal liver-derived macrophage preparation - *Jmjd3* foetal liver-derived macrophages were prepared from embryos at day E14.5 (in a mixed 129SvEv-C57BL/6 background). Embryos were collected from pregnant mice at the indicated day. The foetal liver was removed and kept in Phosphate Buffered Saline (PBS), and the tail was used for genotyping as described above. After knowing the genotype, the liver was meshed by either using the back part of the syringe plunger and passing through nylon mesh (70μm pore size) or aspirating and flushing the minced liver at least 5 times by 22G needle-syringe (until the liver is homogenized). The feotal liver single cells were finally resuspended in 5 ml of conditional medium, plated first on bacterial (non-coated) plates for 2 days, and then transferred to standard cell culture plates for additional 5–6 days before stimulation. LPS from Escherichia coli serotype 055:B5 (Sigma) was used at 10 ng/ml; gIFN (R&D) was used at 10 UI/ml.

2.2 MEFs (Mouse Embryo Fibroblasts) Preparation – MEFs were prepared from 14.5 dpc embryos. Embryos were collected from pregnant mice at the indicated day. The head and hematopoietic system were removed, and the tail was used for genotyping as described in section 1.2.

Embryos were then minced with a clean sterile cutter until the tissue was completely disgregated. The minced issue was then collected in 500 μl of PBS and incubated 5 minutes at 37°C with 500 μl of trypsin. The disgregated cells were finally resuspended in 10 ml of DMEM supplemented with 10% fetal bovine serum (NA), penicillin (100 units/ml), streptomycin (100g/ml), L-glutamine (2mM), Non essential amino acids (0.1 mM) and β-mercaptoethanol (50 μM) and plated on a 10 cm diameter dish.

Cells were grown in 20% oxygen and 5% CO_2 . After almost 2 days when the cells reached confluency, they were splitted once (1:3) and after 3 days, they were frozen in serum additioned with 10% dimethylsulfoxyde (DMSO). Frozen vials were stored in liquid nitrogen up to usage.

Otherwise, cells were directly used for experiments after the first passage in culture.

3. Western Blotting

For western blotting analysis Urea buffer (8M urea, 25mM Tris-HCl;PH 6.8, 1mM EDTA, 10% glycerol) was used to lyse the cells: . Lysed samples were collected by scraping and briefly sonicated on ice, in order to disrupt DNA, before measuring protein concentration. Total cell lysates were assayed for protein concentration with Bio-Rad protein assay. Equal protein amounts (between 20 and 40 μg, depending on the antibodies that were going to be used) were boiled 5 minutes at 95°C in order to denature the proteins, and resolved on a polyacrilamide gel at the desired concentration. Separated proteins were transferred on to nitrocellulose transfer membrane (PROTRAN®), which were then incubated with the desired antibodies.

Primary antibodies were dissolved in 5% BSA in TBS-Tween20 (0.1%)-NaN_3 (0.01%), and horseradish peroxidase (HRP)-conjugated secondary antibodies were dissolved in 5% milk/PBS.

Proteins were finally detected through incubation of the labled membrane with a chemioluminescent substrate (Chemio-Luminescent reagent, Amersham) and exposure to X-ray films.

4. Antibodies

The following antibodies were used:

Anti-Jmjd3 rabbit polyclonal antibody, produced by Abgent (San Diego, CA, USA), used 1:500 in WB

Allophycocyanin (APC) anti-mouse CD45.2, eBioscience, used 1:200 in flow cytometry

Fluorescein isothiocyanate (FITC) anti-mouse CD45.1, eBioscience, used 1:100 in flow cytometry

5. qPCR Analysis

Total RNA was extracted from indicated mouse tissues using TRIzol solution (Invitrogen) according to the instructions specified by the manufacturer.

The extracts were quantified by spectrophotometer (Nanodrop). cDNA synthesis was performed using M-MLV reverse transcriptase (FINNZYME, Finland), using random primers. For the reverse transcription, 1μg of total RNA were used.

Mix 1X for RT-PCR	
Total RNA	1μg
10X MMLV buffer	2μl
dNTPs (10mM)	1μl
Random primers (50μM)	1μl
MMLV reverse transcriptase	1μl
ddH_2O	Up to 20μl

RT-PCR program that was used is coming below:

Temperature	Time
25°C	10 min
42°C	45 min
95°C	5 min
4°C	pause

After the cDNA synthesis was performed, 80µl ddH2O was added to the samples and mixed well. We used this mix to make the qPCR reactions.

Mix 1X for qPCR	
cDNA	5µl
Primers (forward+backward)	0.2µl
SYBR 2X	10µl
ddH_2O	4.8µl

A list of primers using in qPCR is available below.

Primer sets	Forward Primer (5'-3')	Backward Primer (5'-3')
JD3F/B	ACC ACC ATC GCT AAA TAC GC	ACC TCT TGG CAT CAG ACA GG
GYS1F/B	TGT CCT CCA CCA GCC CTC TAT	GGA GAG GTT TGT AGT CAC ACT G
PCK1F/B	TGC CTG GAT GAA GTT TGA TGC	TCC AGG AGG TGA TGG TGA CT
PPAR1F/B	TCC ATC GGT GAG GAG AGC TCT	GCG TGA ACT CCG TAG TGG TAC
G6PC1F/B	GCG CAG CAG GTG TAT ACT ATG	AAG TGA GCA GCA AGG TAG ATC
GLUT4F/R	CTA CGC CAC CAT AGG AGC T	GAG ACA TAG CTC ATG GCT GGA
ALBF/R	AGC TGA GAC CTT CAC CTT CCA	AAG CAG GTG TCC TTG TCA GCA

6. Mass Spectrometry analysis of *Jmjd3*$^{-/-}$ MEFs

6.1 Harvesting of the cells - *Jmjd3*$^{+/+}$ and *Jmjd3*$^{-/-}$ MEFs were plated on 10-cm tissue culture plates. The cells were trypsinized and harvested according the routine protocol.

Every 10^7 MEF cells were divided in to a 50ml Falcon tube and pelleted for 10 min at 1200 rpm (4°C). The cells were resuspended in 10 ml cold PBS and spun down for 10 min at 1200 rpm (4°C) and the supernatant were removed.

6.2 Preparation of nuclei – Each cellular pellet was carefully resuspended in 7.5 ml N-Buffer (10% Sucrose, 0.5 mM EGTA;PH=8.0, 60 mM KCl, 15 mM NaCl, 15mM HEPES;PH=7.5, 30µg/ml Spermine, 0.5 mM PMSF, 0.2 mM Pefabloc, 5 µg/ml Aprotinin, 5 µg/ml Leupeptin, 5 µg/ml Pepstatin A, 1mM DTT, 5mM NaButyrate, 5mM NaVanadate, 5mM NaF) . 0.5% Triton-X solution was added to the samples. The tubes were rolled for 10 min at 4°C.

The content of each tube carefully poured onto the sucrose cushion (avoid mixing the sample with the cushion). The nuclei were spun down at 3750 rpm for 30 min. Supernatant were removed. The pellet was resuspended in ice-cold PBS. The nuclei were spun down at 4000 rpm for 20 min. The supernatant was removed.

6.3 Acididic Extraction of core-histones - The pellets were resuspended in ice-cold PBS (approx 2 ml per each cushion, this volume might vary with the pellet volume). Equal volume of 0.8N HCl were added to the samples. The tubes were rolled O/N at 4°C.

The samples were spun at 13000 rpm for 10 min. The supernatant were collected and pooled together. The pooled supernatant was dialyzed in 0.1 M CH3COOH ice-cold for 16-20 hours. The dialyzed samples were collected and aliquoted about 1 ml in Eppendorf tubes. The samples were kept at -20°C.

6.4 Analysis and quantification of core-histones – The sample in each eppendorf tube was resuspended in 50 µl H_2O. Bradford assay and SDS-PAGE were performed to evaluate the purity and amount of the samples. Then the samples were digested by Arg-C (Arginase) and run on Mass Spectrometry instrument.

7. Salmonella infection of *Jmjd3*$^{-/-}$ macrophages

7.1 Foetal liver-derived macrophage preparation - Feotal liver cells were plated at 150,000 cells/well in 6-well tissue culture plates in a conditional medium deferentiating the cells toward macrophages (protocol described at section 2.1). The day before Salmonella infection, the medium was replaced with 2 ml of Dulbecco's modified culture medium (DMEM), supplemented with 10% of fetal bovine serum of Nourthern American origin, without L929 conditional medium and without pen/strep. The cells were treated with 2 ml/well of recombinant interferon-γ (100 units/ml).

7.2 Salmonella culture – Salmonella typhimurium (ATPGEX; Ampicilin resistant) were inoculated in 10 ml LB containing ampicilin and incubated O/N at 37°C. On the day of infection, three different dilutions of culture (1:10, 1:20 and 1:50) were prepared. We had to check the OD. Of the bacterial culture because we needed to have a bacteria at the logarithmic phase for the infection. The proper OD is ~0.6. The number of bacteria calculated according the following formula:

$$\text{Number of bacteria per ml of culture} = Ab_{600} \times 10^{9}$$

With this number and with the desired M.O.I which we need for the infection, we can calculate that how much of the culture contained the bacterial numbers which we need. For example, if we need 25 salmonella for each cell of macrophage and if we assume that the OD for the culture is 0.6. As we have 150,000 cells in each well, then:

$$25 \times 150{,}000 = 3{,}750{,}000$$

We need 3,750,000 salmonella for each well. We have 0.6×10^9 salmonella in 1 ml of LB. We need to add x µl of LB containg Salmonella in to each well of the cells:

$$x=3750000\times1000/6\times10^8$$

7.3 Salmonella infection – The needed number of salmonella cells were diluted in Dulbecco's modified Eagle's medium (DMEM) supplemented with 10% fetal bovine serum of Nourthern American origin, without L929 conditional medium and without pen/strep. After macrophage cells were washed twice with 2 ml/well of PBS, 500 µl of the salmonella in DMEM was added in each well with a multiplicity of infection (MOI) of 25. To increase the uptake of salmonella, plates were centrifuged at 1500 rpm for 2 sec. Uptake of salmonella was allowed to occure for 1 hr. at 37°C. After cells were washed once with DMEM without pen/strep to remove the salmonella that were not taken up by the cells, 500 µl of DMEM without pen/strep containing 1X gentamicin was added to each well and incubated at 37°C for 1hr.

7.4 Isolation of salmonella cells - This time point was considered as 0 h time point in this study. Before lysis of the macrophages, warm PBS was used to remove gentamicin. Macrophages were lysed in 1 ml 1% Triton X-100 in PBS for different time points. Serial dilutions were plated on LB agar plates and incubated at 37°C overnight and the resulting salmonella CFUs seen on LB plates were counted.

8. Adoptive Transfer of knockout foetal liver cell

We set out to transf knockout foetal liver cells in to irradiated recipient mice which leads to the generation of chimeras carrying the genetic mutation restricted to cells of the haematopoietic system (*haematopoietic* chimeras). With this strategy, we can define the effect of the *Jmjd3* absence in the *haematopoietic* system.

8.1 Lethal Irradiation – One day before irradiation, the mice had to be feed with water containing Ampicilin (1mg/ml). The C57BL/6-Ly5.1 mice were used as recipients and irradiated with 7.25Gy (8 minutes) irradiation with γ-irradiator (This amount of irradiation had to be scheduled manually because there was not any planned program on the machine.)

8.2 Foetal Liver cell preparation – Foetal liver were dissected from XB814 strain embryos at day E14.5 (in a mixed 129SvEv-C57BL/6 background). Embryos were collected from pregnant mice at the indicated day. The foetal liver was removed and kept in Phosphate Buffered Saline (PBS), and the tail was used for genotyping as described above. After knowing the genotype, the liver was meshed by either using the back part of the syringe plunger and passing through nylon mesh (70μm pore size) or aspirating and flushing the minced liver at least 5 times by 22G needle-syringe (until the liver is homogenized). The cells have to be counted and washed 2X with PBS (Spin 1200 rpm, 5 min; aspirate and resuspend).

8.3 Intravenous Injection – 3×10^{6} foetal liver cells were resuspended in 200μl PBS and 100μl of that were injected intravenously through the tail vein to each mouse.

8.4 Reconstitution Efficiency Checking – Reconstitution efficiency examined ~ 6 weeks after transfer. For this purpose, we obtained 5-6 drops of blood from the mouse-tail and kept it in an eppendorf tube containing 1-2 µl of heparin. 10 µl of blood were transferred in to each well of 96 well plate containing 150 µl PBS. Blood were mixed by pipeting up and down. The blood cells were spin down for 5 sec at 2000 rpm at 4°C. The supernatant were aspirated. Then the Red Blood Cells were lysed by RBCL solution. For this step, 50 µl of RBCL solution added to each well and incubated fro 3 min on ice. 150µl PBS added in to the wells containing RBCL and mixed. The plate were spined down and supernatant was aspirated. Washing step by RBCL were repeated until the pellet became white. Obtained cells were stained with anti-Ly5.1 and anti-Ly5.2 antibodies for 20 min and acquired by FACs machine.

RESULTS

1. Generation of *Jmjd3* constitutive knockout mice :

1.1. The integration site of the gene trap vector – In the PCR designed to identify the insertion point of the trap cassette (section 1.1.1 in Methods & Material), all four primer pair combinations yielded a PCR product. The closer the forward primer with respect to the trap cassette, the shorter the PCR product, which confirmed that the insertion had indeed occurred in Jmjd3 and indicated that the insertion point is in the 3' region of intron I (Figure 9). The shortest amplicon was cloned into a pCRII-TOPO plasmid vector and subsequent sequence analysis identified the insertion point of the gene trap vector at position 4187 of intron I.

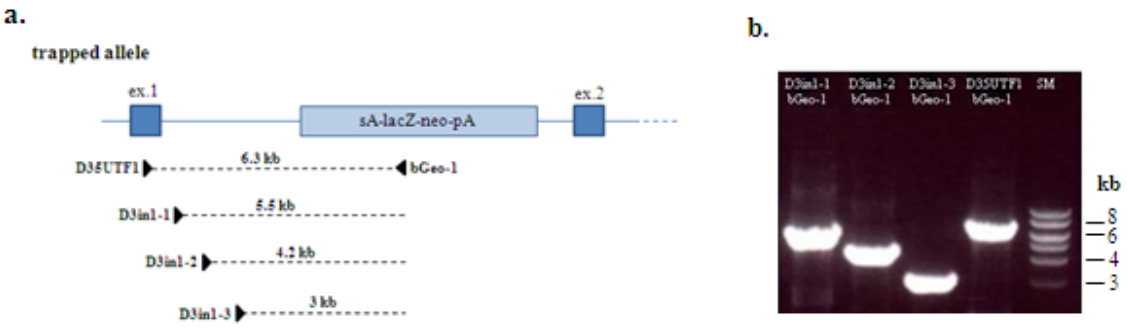

Figure 9. Identification of the insertion site of the gene trap vector by PCR. Four forward primers, annealing to different regions in exon one and intron one, respectively, were used in combination with a reverse primer located in the trap cassette. All PCR reactions yielded a product, which was progressively shorter the further downstream the forward primer annealed in intron one, demonstrating that the insertion of the trap cassette had occurred in the 3' region of intron one.

The integration site is downstream of the first exon near the already mapped NF-κB binding sites (De Santa, Totaro et al. 2007) and in a region marked by H3K4me3 (Figure 10).

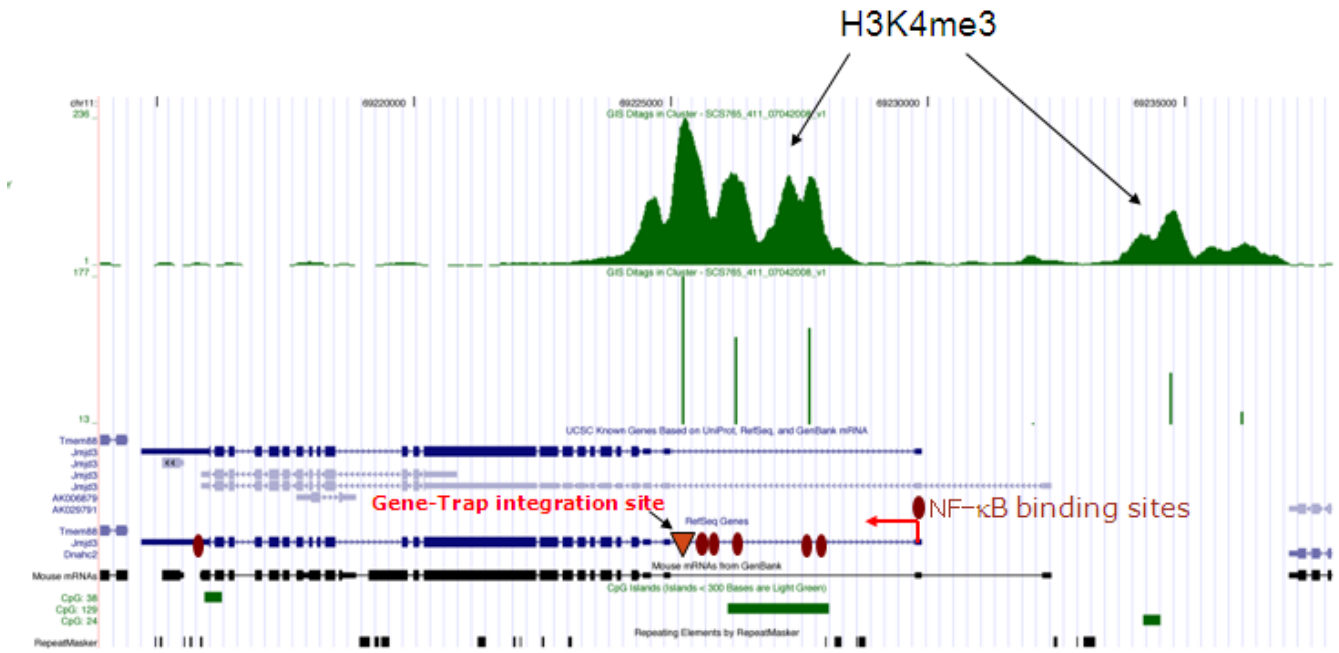

Figure 10. Integration site of the gene trap cassette in *Jmjd3* gene. The insertion site is located clos to NF-κB binding sites. Moreover, at this area H3K4me3 mark which is a mark of transcription activation is detected.

1.2. Genotyping strategy for the trapped *Jmjd3* allele. I designed a triplex genotyping PCR in which the wild-type allele generates a 282-bp band, while the KO allele generates as a 259-bp band. The pattern could be easily distinguished on a 3% agarose gel (Figure 11).

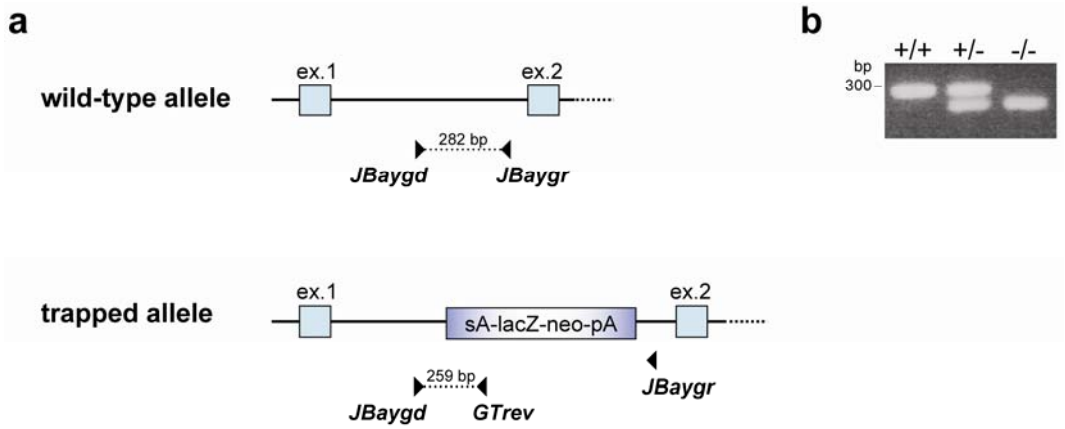

Figure 11. Genotyping of the Jmjd3 gene trap allele. (a) A triplex PCR-based strategy was used to identify the Jmjd3 gene trap allele. The scheme shows the position of the three primers. **(b)** The primer pair JBaygd/JBaygr amplified a 282 bp product from the wild-type allele , whereas the theoretical product of 11.7 kb

from the trapped allele was not amplified. The primer pair JBaygd/GTrev yielded a 259 product only from the trapped allele.

1.3. Generation of the XB814 mouse line - The XB814 mouse line was generated by injecting XB814 gene trap ESCs into C57BL/6 blastocysts. One male chimera with rather low level of chimerism (<30%) transmitted the mutant allele through the germline. Heterozygous mice obtained this way were then crossed to wild-type C57BL/6 females. Germline transmission was confirmed by PCR analysis on genomic DNA extracted from tail biopsies (Figure 11b). All experiments described in this thesis were carried out on mice with a L129; C57BL/6 mixed background.

1.4. Perinatal Lethality in Jmjd3$^{-/-}$ Mice - Genotyping PCR analyses of the three weeks-old progeny from heterozygous crosses between Jmjd3$^{+/-}$ mice revealed the complete absence of any Jmjd3$^{-/-}$ offspring, suggesting embryonic or perinatal lethality. To more accurately pinpoint the time of disappearance of Jmjd3$^{-/-}$ mice, embryos were harvested at various stages of development and genotyped by PCR. Although we observed the expected Mendelian frequency of Jmjd3$^{+/+}$, Jmjd3$^{+/-}$, and Jmjd3$^{-/-}$ offspring throughout embryonic development , all *Jmjd3*$^{-/-}$ mice died within the first 48 hrs after birth (Table 2). For precise monitoring and to distinguish the reason of death, timed breeding between heterozygous mice were set up and neonates were monitored carefully from the moment they were born. Special care was taken to disturb the delivery process as little as possible and to avoid any additional stress for the mother. Immediately after the delivery, neonates were briefly separated from the mother and small tail biopsies were taken for genotyping. The neonates were marked by injecting subcutaneously a drop of Indian ink. This strategy enabled us to genotype and monitor each pup immediately after delivery. The analysis showed that about 70% of all homozygous mutants were born dead or died within minutes of delivery and only

30% of the mutants survived the first few hours. Among the 12 mutants being followed, two were alive for about 24 hrs which was the longest survival time observed. All the dead delivered pups were *Jmjd3*$^{-/-}$ except one *Jmjd3*$^{+/-}$ which indicated that the perinatal lethality could be entirely ascribed to the homozygous mutants.

Table 2. Frequency of Jmjd3$^{+/+}$, Jmjd3$^{+/-}$, and Jmjd3$^{-/-}$ embryos during development

	Number of animals/genotype			
Age of embryos (post coitum)	+/+	+/-	-/-	Frequency of -/- mice
10.5 d	4	16	6	23%
12.5 d	4	7	5	31%
14.5 d	6	6	5	29%
Age of newborn (post partum)				
1 d	11	19	4	12%
2 d	9	14	0	0

Embryos from timed matings were genotyped on embryonic day 10.5, 12.5, 14.5, or 1 d and 2 d post partum. Far right column shows the observed percentage of *Jmjd3*$^{-/-}$ mice (the predicted Mendelian percentage is 25%).

Although the *Jmjd3*$^{-/-}$ mice displayed no overt anatomical defects, they were generally paler in their skin colour and looked lethargic and in any case much less reactive than their littermates. They were hunched and suffered of sudden bouts of cramped movements,

resembling a gasping behaviour due to efforts to breathe. The heartbeat, as monitored through the skin, was non-rhythmic and none of the mutant pups showed an apparent milk spot, indicating the lack of feeding (Figure 12).

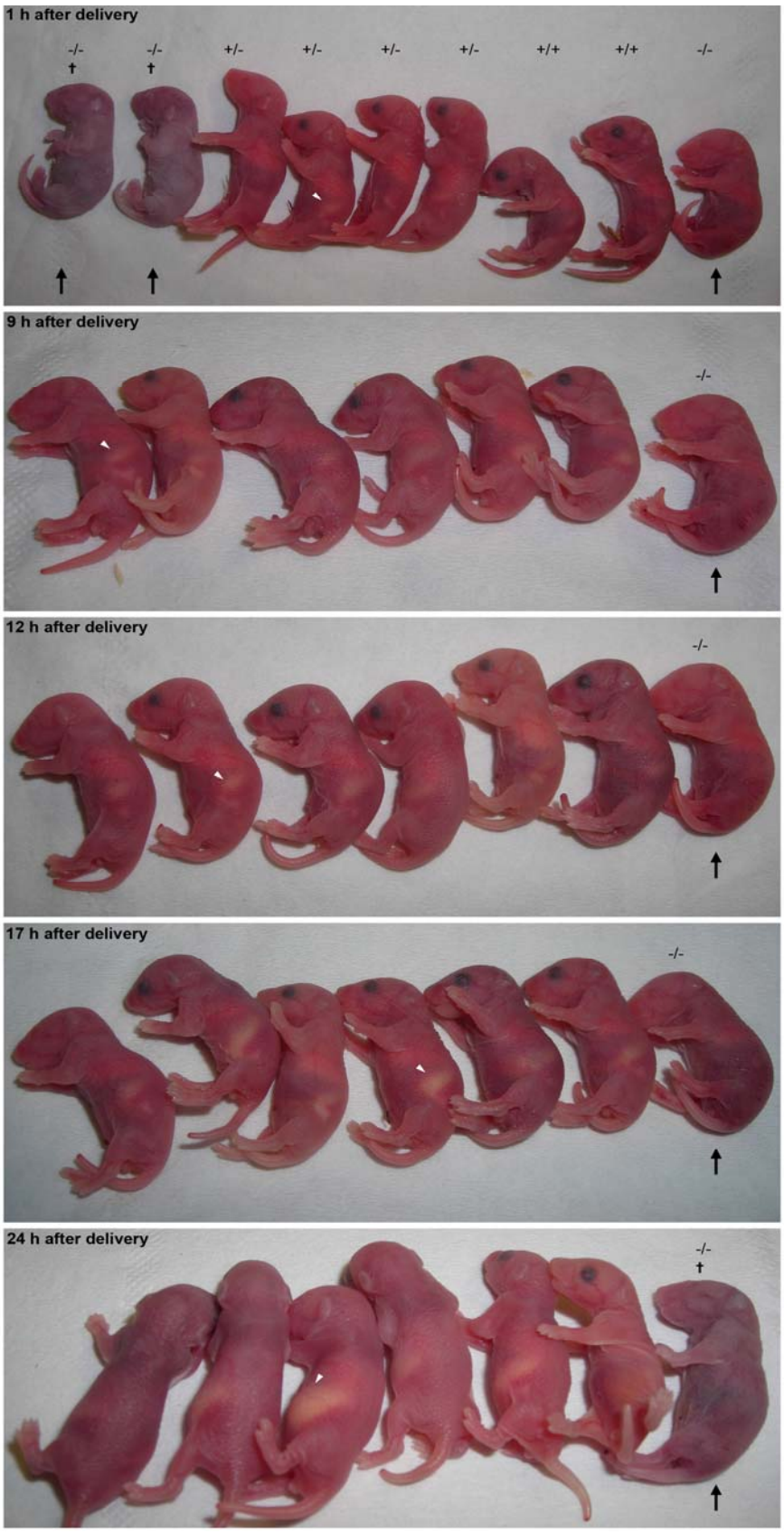

Figure 12. Perinatal lethality in *Jmjd3*$^{-/-}$ mice. None of mutant pups showed an apparent milk spot, indicating the lack of feeding.

In conclusion, *Jmjd3*$^{-/-}$ mice can develop apparently normally and reach birth but they die soon after delivery.

1.5. *Jmjd3* expression during mouse embryonic development - To identify the cause of the perinatal lethality in *Jmjd3*$^{-/-}$ mice, we first determined the expression of *Jmjd3* during embryonic development in different tissues. For this purpose, *Jmjd3* expression was analyzed by *in situ hybridization* (ISH). For detecting the Jmjd3 transcript, an anti-sense probe complementary to the 3' region of the Jmjd3 locus and spanning exons 19-23 was used. ISH was performed on sagittal and coronal embryo sections of various developmental stages between E9.75 and E16 (Figure 13).

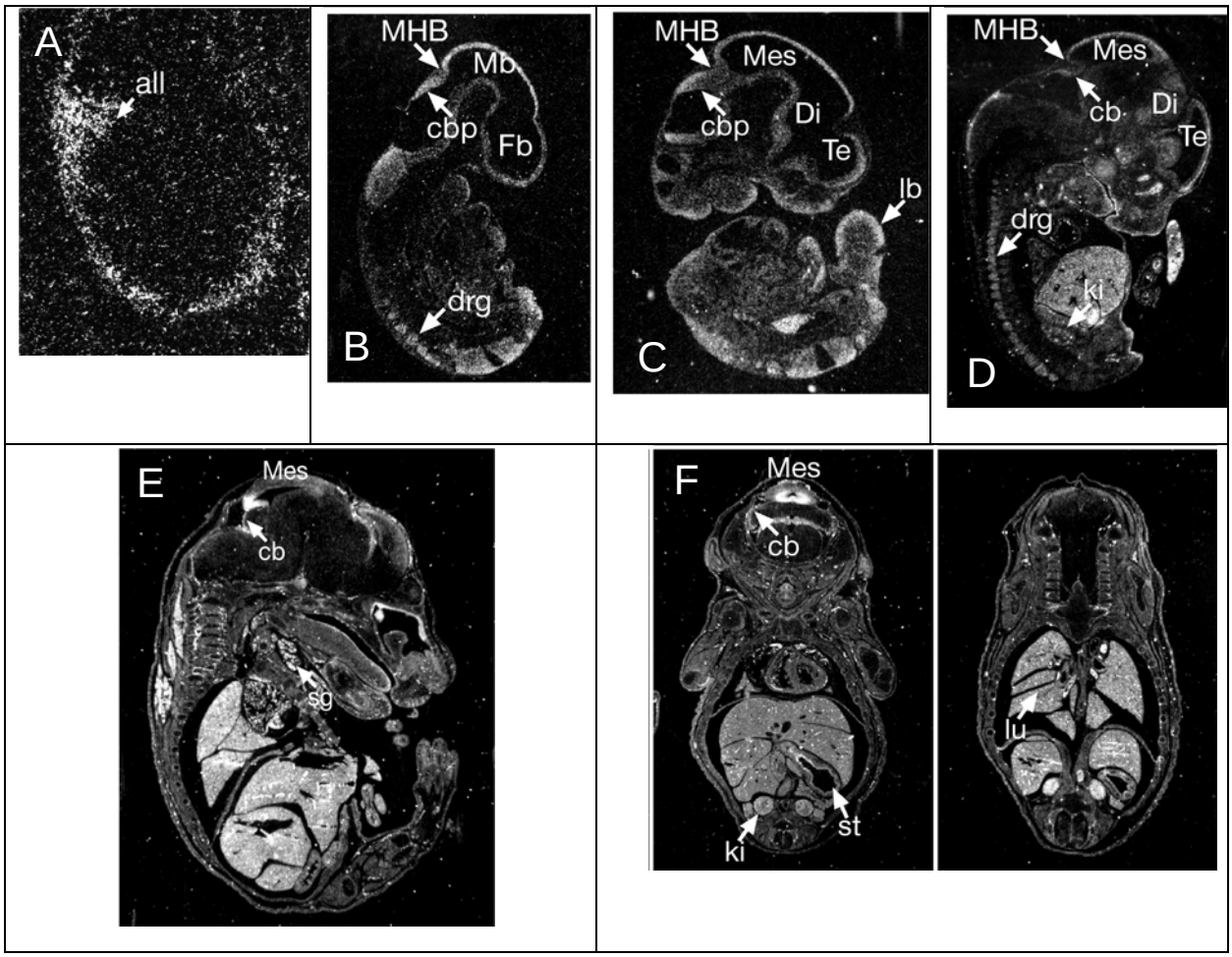

Figure 13. Localization of *Jmjd3* transcripts in mouse embryos analyzed by *in situ hybridization*. A. In the E7.5 embryo, *Jmjd3* is expressed in the allantois (all). **B.** E9.75 **C.** E10.75 and **D.** E12.5 embryo showing *Jmjd3* expression in the midbrain-hindbrain border (MHB), cerebellar primordium (cbp), midbrain (Mb), forebrain (Fb), dorsal root ganglia (drg), diencephalon (Di), telencephalon (Te), limb bud (lb) and kidney(ki). **E,F.** *Jmjd3* expression in cerebellum(cb), salivary gland (sg), kidney (ki), stomach (st) and lung (lu) in the E16 embryo.

This result showed the evident expression of *Jmjd3* in all three primary brain vesicles of the neural tube, the hindbrain (Hb), the midbrain (Mb) and the forebrain (Fb) and also in cerebellar primordium (cbp) at day E9.75 (Figure 13b). At day E10.75, the general expression pattern remained constant with notable expression in the developing central nervous system (CNS) in particular the mesencephalon (Mes), the diencephalon (Di) and the telencephalon (Te). From E12.5 to E16, during the peaks of neurogenesis, Jmjd3 expression was maintained in the CNS with the highest levels in cerebellum (cb) and mesencephalon (Mes).
Overall, this analysis showed that Jmjd3 was expressed throughout the developing mouse CNS.

1.6. *Jmjd3* expression in knockout tissues – Expression analysis of Jmjd3 in knock-out cells and tissues was assessed to determine if the insertion of the gene-trap results in the complete loss of Jmjd3 expression in all the mouse tissues. RT-qPCR showed that in fact Jmjd3 expression is selectively abrogated in some but not all tissues, suggesting that this is in fact a hypomorph and not a full knock-out (Figure 14). For example, the expression of Jmjd3 in the brain, lung and liver of the knock-out mice was almost abolished. But for some tissues such as heart, intestine, spleen and skin, Jmjd3 expression was still present in knock-out mice.

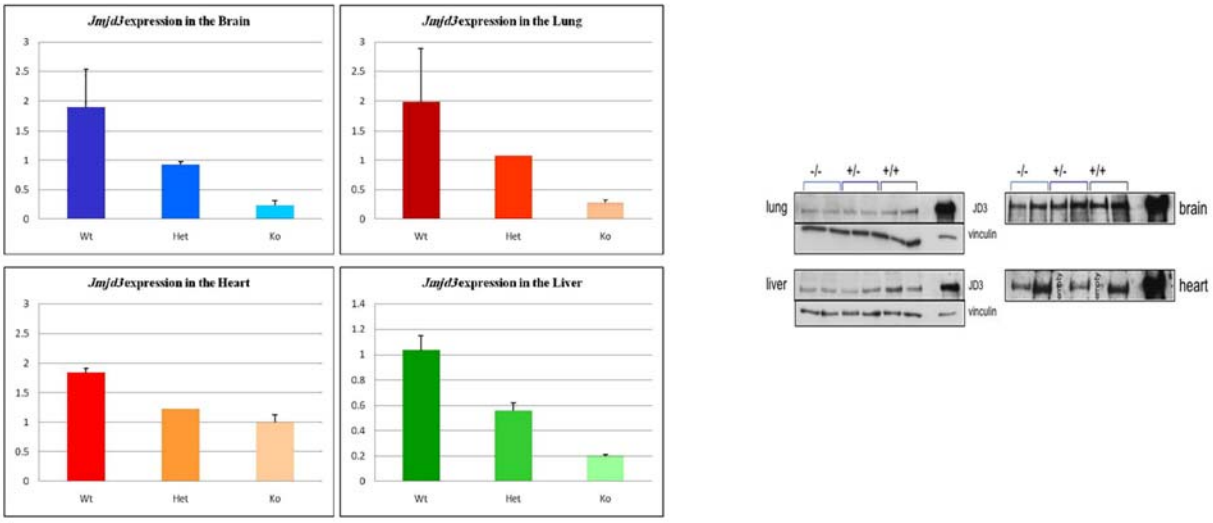

Figure 14. *Jmjd3* profile in different mouse tissues from wt, heterozygous and homozygouns mutants at the mRNA level (left) and at the protein level (right). For some tissues such as brain and lung, Jmjd3 was almost depleted in the knockout pups and in some such as heart and liver, Jmjd3 was still present in knockout pups at the mRNA level. Jmjd3 protein was present in all tissues even in knockout pups.

Unexpectedly, Jmjd3 was present at the protein level in all the analyzed tissues which could be due to the stability of Jmjd3 protein.

There was a complete loss of Jmjd3 expression in myeloid cells such as fetal liver-derived macrophages (Figure 27).

1.7. Histological analysis of Jmjd3 mutants – To investigate the cause of lethality in Jmjd3 mutants, we performed a thorough histological examination of the main vital organs. To do this, wild-type and homozygous mutant neonates were fixed in 4% formaldehyde immediately after birth and further processed for hematoxylin and eosin (H&E) staining on serial sections. In the skin, well differentiated subdermal, dermal, and epidermal layers were detected. Keratinocyte differentiation appeared normal in all regions of the skin, tongue and aglandular stomach, and no differerences were seen between wild type, heterozygous and knockout tissues. We therefore excluded that defects in skin barrier function could cause perinatal lethality through transepidermal water loss. There were no

malformations or abnormalities in the entire gastrointestinal tract that could lead to feeding, digestion or absorption difficulties. The musculoskeletal system and the peripheral respiratory apparatus, including lungs, ribcage and diaphragm were also free from alterations in morphology or architecture. liver and the hematopoietic organs, bone marrow, spleen and thymus appeared also to be normally developed (data not shown). Conversely, histological analysis of the brain revealed that the cerebellar cortex of Jmjd3$^{-/-}$ newborn mice had a moderate decrease in foliation in comparison to wild-type littermates (Figure 15).

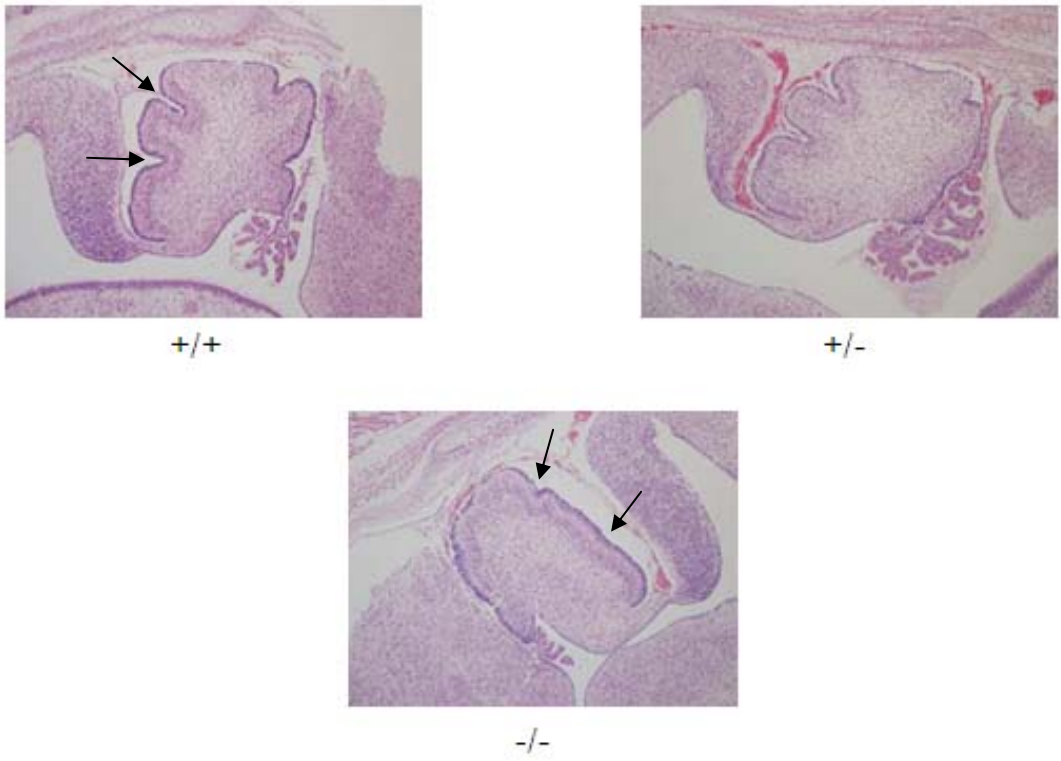

Figure 15. Cerebellar afolia in Jmjd3 mutants - H&E staining on sections of cerebellum region of newborn Jmjd3$^{+/+,}$ Jmjd3$^{+/-}$ and Jmjd3$^{-/-}$ mice.

This mutant phenotype showed a variable penetrance and, although it indicated the possible existence of relatively mild brain developmental defects, it could not account for the neonatal lethality of the homozygous mutant mice.

We therefore explored other possible causes of perinatal lethality. As mentioned before in contrast to their siblings, some of the mutant neonates had little or no milk in their stomachs and looked paler. This led us to hypothesize that the mutant may not compete for nourishment probably because of lack of energy. Impaired energy homeostasis in neonates is one of the possible reasons of perinatal lethality (Wang, Finegold et al. 1995). Around birth drop in glucose levels due to the disconnection from placenta is counteracted by increased glycogenolysis and neoglycogenesis in the liver. The rate-limiting enzyme in neoglycogenesis is PEPCK (Phosphoenol Pyruvate Carboxy Kinase), whose expression is upregulated in the liver just before birth (Hanson and Reshef 1997) (Hume, Burchell et al. 2005) (She, Shiota et al. 2000) (Nordlie, Foster et al. 1999) (Hanson and Reshef 2003). Any disruption in this phenomenon can cause defects in energy homeostasis and lead to lethality in the newborn pups. We therefore set out to determine a) glucose levels in newborns, and b) the expression of enzymes involved in glycogenolysis and neoglycogenesis. Among the enzymes that have a role in glycogenolysis and neoglycogenesis, we checked the expression level of Glycogen Sinthase (GS), PEPCK, Glucose-6-phosphatase (G6Pase), Glucose transporter 4 (GLUT4) and Albumin in the liver taken from the newborn pups. Only the expression level of PEPCK was downregulated in *Jmjd3*$^{-/-}$ pups comparing to wild type and heterozygote pups (Figure 16).

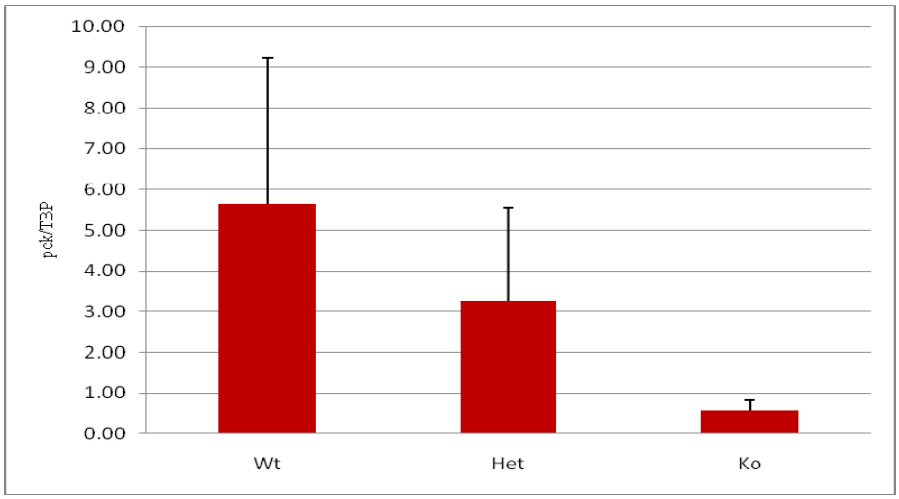

Figure 16. PEPCK expression level in wt, Het and KO neonates (Number of mice: Wt=2, Het=3 & KO=3). PEPCK expression was downregulated in Jmjd3$^{-/-}$ pups comparing to wild type and heterozygote pups.

Phosphoenolpyruvate carboxykinase (PEPCK) is a key enzyme in the synthesis of glucose in the liver and kidney and of glyceride-glycerol in white adipose tissue and small intestine. This enzyme is absent in fetal liver but produced at birth, concomitant with the capacity for gluconeogenesis (Hanson and Reshef 2003). In parallel with testing the expression levels of the mentioned enzymes, we checked also the glucose level in the neonates. Glucose levels were normal in the neonates suggesting that the drop in PEPCK was not causing a drop in glucose levels (Figure 17).

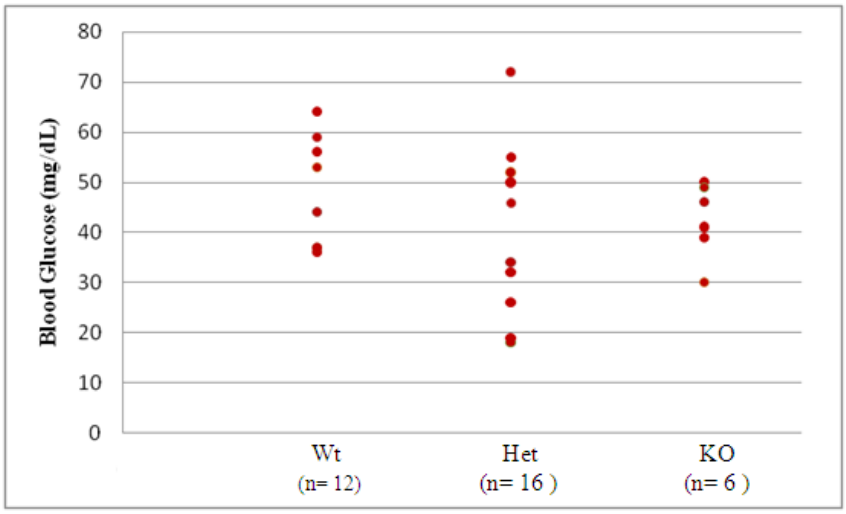

Figure 17. Blood glucose level in neonates; normal glucose level was seen in ko neonates.

We reasoned that maybe the reduction in PEPCK was a response to the pathological changes occurring in the *Jmjd3*$^{-/-}$ mice. We checked in the literature and found that PEPCK levels are downregulated in hypoxia, which suggested the possibility of a respiratory dysfunction in this perinatal phenotype (Pison, Chauvin et al. 1998).

1.8. Respiratory failure in Jmjd3 mutants – We performed physiological and histological analyses for the respiratory system in collaboration with Gérard Hilaire (CRN2M, Marseille, France). Embryos were taken out from uterine horns at E18.5 and assessed for their respiratory activity by recording *in vivo* breathing-associated pressure changes (plethysmography). *Plethysmography* is a test used to measure changes in air volume in the lung and define how much air can be held in the lungs. Wild-type and heterozygous mice, immediately upon exteriorization, initiated breathing in a gasping-like behaviour for 2-5 min, which was characterised by deep respiratory movements at a low frequency (about 2-5 c·min^{-1}) involving the entire body muscles and including wide mouth opening. Thereafter, they produced normal robust respiratory cycles at a faster rhythm (Jmjd3$^{+/+}$: 46 ± 7 c·min^{-1}, n = 10; Jmjd3$^{+/-}$: 45 ± 30 c·min^{-1}, n = 2). In contrast, all mutant neonates (n = 8) failed to show any signs of ventilation or respiratory efforts, like gasping, and died shortly after exteriorization (Figure 18).

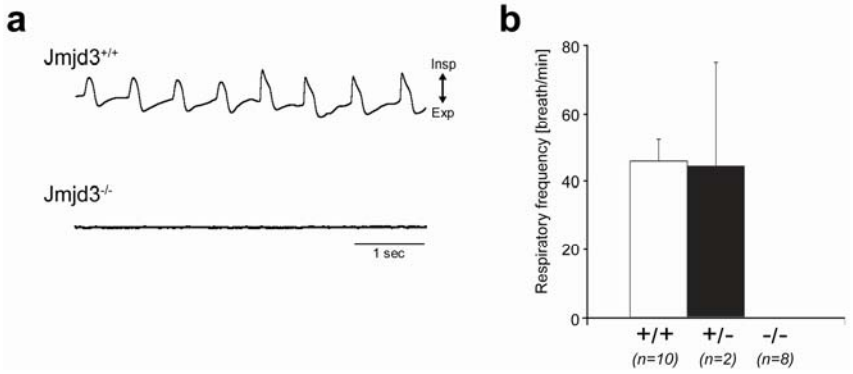

Figure 18. Whole-body plethysmographic recording in Jmjd3$^{+/+}$, Jmjd3$^{+/-}$ and Jmjd3$^{-/-}$ embryos. The mutant neonates did not show any sign of ventilation and died shortly after taking out from uterine horn.

To exclude that the primary cause for perinatal death could have been a heart failure which in turn could have determined respiratory failure, we recorded electrocardiograms of embryos *in utero* (Figure 19) . At E18.5, the heart was beating in both Jmjd3$^{+/+}$ (61 ± 9 c·min^{-1}, n = 6) and Jmjd3$^{-/-}$ (102 ± 17 c·min^{-1}, n = 5) embryos, thus excluding heart failure as a cause of the perinatal phenotype of the mutants.

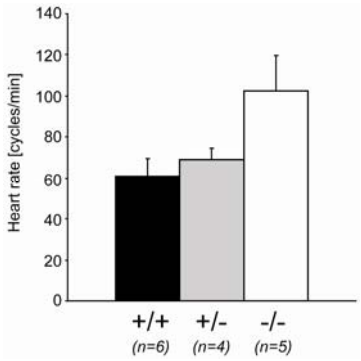

Figure 19. Heart beating records in Jmjd3$^{+/+}$, Jmjd3$^{+/-}$ and Jmjd3$^{-/-}$ embryos. Normal electrocardiograms were recorded for jmjd3$^{-/-}$ embryos.

Next, we assessed whether muscular or neuromuscular dysfunctions could cause the lack of ventilation in Jmjd3 mutants. Single electrical shocks were applied to the diaphragm or the phrenic nerve of either exteriorised or in *utero* embryos at E18.5. Electrical stimulations of the diaphragm or the phrenic nerve induced diaphragmatic contractions in both wild type and mutant embryos.

1.9. Defect in the respiratory rhythm generator in Jmjd3 mutants at E18.5 – No functional anomalies in the peripheral respiratory and cardiac systems led us to considering a central respiratory defect. We therefore examined the respiratory rhythmic activity generated *in vitro* by the central respiratory network isolated in *en-bloc* brainstem preparations at E18.5. In preparations of wild-type (n = 6) and heterozygous (n = 14) embryos, rhythmic bursts of

potentials were detected from the cervical phrenic roots at a phrenic burst frequency of 12 ± 4 $c \cdot min^{-1}$ and 8 ± 1 $c \cdot min^{-1}$, respectively. Recordings performed on Jmjd3 mutant preparations (n = 8) revealed the absence of any rhythmic or tonic phrenic nerve activity (Figure 20).

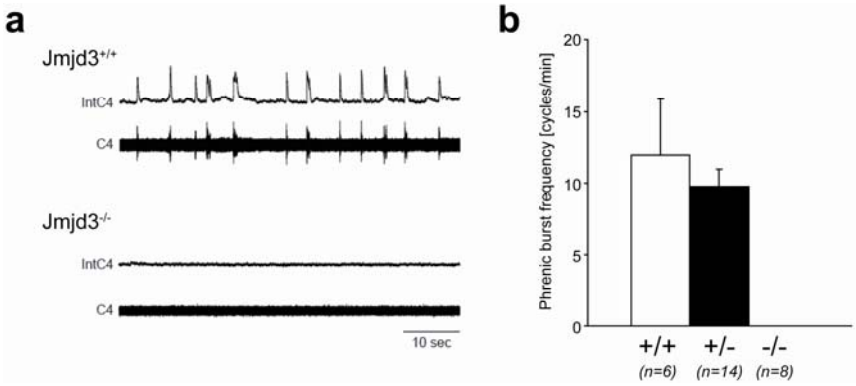

Figure 20. Phrenic burst frequency records in Jmjd3$^{+/+}$, Jmjd3$^{+/-}$ and Jmjd3$^{-/-}$ embryos. Rhythmic or tonic phrenic nerve activity was not detected for Jmjd3 mutants.

The lack of rhythmic phrenic bursts in Jmjd3$^{-/-}$ embryonic preparations could be the consequence of a defect either in respiratory rhythmogenesis or in synaptic transmission of the medullary respiratory drive to the cervical phrenic motoneurons or in a combination of both defects. (Figure 21) The phrenic motoneurons responses to spinal synaptic inputs were analysed *in vitro.* The respiratory output pathways running from the medulla towards the phrenic motoneurons were activated by applying single electrical shocks to the spinal cord within the ventromedial and the ventrolateral spinal columns at the level of the second cervical segment. Each electrical shock induced a short latency response of the C4 phrenic motoneurons in both wild-type and mutant preparations. This analysis demonstrated that the C2-C4 pathway was functional and phrenic motoneurons were able to respond to spinal synaptic excitation in Jmjd3$^{-/-}$ mutants.

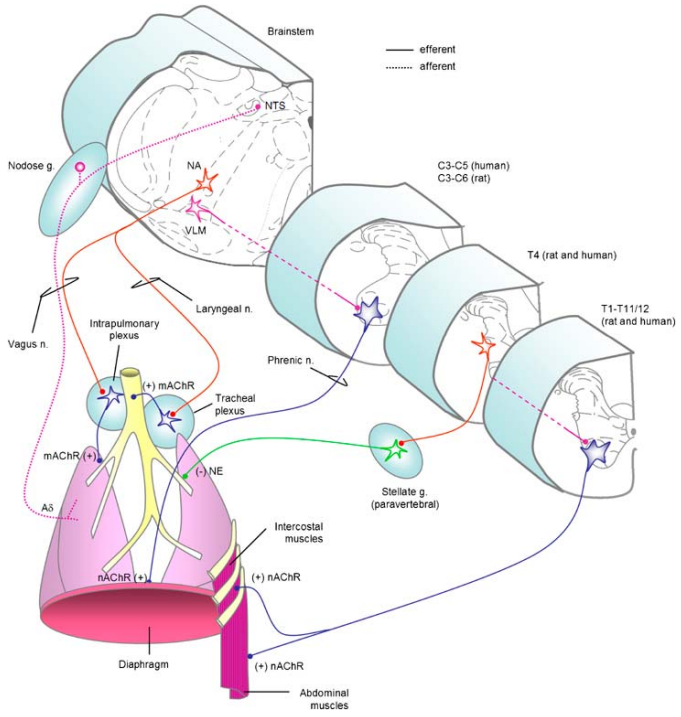

Figure 21. Schematic representation of respiratory neurons in the main brainstem regions

Second, to assess whether the phrenic motoneurons were responsive to synaptic inputs from the medulla, we applied single electrical shocks to the medulla at the level of the ventral respiratory column (VRC). Electrical stimulation of the VRC applied during expiration shortened the expiratory period, triggered a phrenic inspiratory burst and reset the phase of bursts in wild-type preparations. By contrast, in mutant preparations single-shock electrical stimulation of the VRC did not induce a phrenic burst. Together these results showed that the VRC, when activated, could induce sustained discharges of the phrenic motoneurons, indicating that the synapses and the pathway between the medullary respiratory centres and the phrenic motoneurons were functional in Jmjd3$^{-/-}$ preparations. Given the ability of phrenic motoneurons to be activated by spinal as well as medullary synaptic inputs, the lack of C4 rhythmic bursting activity in Jmjd3 mutant mice was an indication for a silent or defective respiratory rhythm generator (RRG). The fact that no rhythmic respiratory phrenic bursts were detected during and after the long-lasting discharge induced by electrical shocks applied to the

rostral ventrolateral medulla or raphe area, suggested a defective rather than quiescent RRG in Jmjd3$^{-/-}$ neonates.

Normal respiratory rhythm in mammals is generated by NK1R neurons in the PreBötzinger complex (preBötC).

Thomas Burgold from Giuseppe Testa group performed more detailed experiments to see if the Jmjd3$^{-/-}$ mutants have any abnormality in the formation of NK1R neurons in preBötC complex and they managed to show that defects in the generation of these neurons in Jmjd3$^{-/-}$ mice perturb normal breathing rhythm and is the main cause of respiratory problems and perinatal lethality in Jmjd3 mutants.(More details can be found in Thomas Burgold's thesis.)

2. The impact of Jmjd3 absence on histone methylation in *Jmjd3*$^{-/-}$ MEFs and macrophages using mass spectrometry

Mass spectrometric approaches developed for analysis of histone post-translational modifications (PTMs) over the past decade. Traditional technique for studying histone PTMs is an immunoassay using site-specific antibodies. However, antibodies are costly and cumbersome to generate. In addition, the simultaneous presence of multiple modificstions lead to epitope occlusion and more importantly, antibodies alone cannot be employed to identify novel modification sites. Conversly, mass spectrometry can determine the exact location of the PTM and acts as a complimentary and improved technique in PTMs analysis.

A major challenge in this field is the presence of different modifications that results in a complex mixture of multiply modified isoforms. For example, a H3 histone peptide of residues 6-20, TARKSTGGKAPRKQL, contains three potential lysine sites which can be acetylated or mono-, di-, or tri-methylated. There are also two potential arginine sites which

may be mono- or di-methylated and three potential phosphorylated sites (two threonines and one serine). Therefore, a total of eight modifications can occur concurrently or in various combinations. In spite of being only a 15-mer pepride, more than 100 potential isoforms of this peptide can be present in a sample. Hence, the mass spectrometer being coupled directly to a high pressure liquid chromatography (HPLC), gas chromatography (GC) or capillary electrophoresis (CE) separation column to separate the sample in to a series of components which then enter the mass spectrometer sequentially to simplify the mixture. The samples are ionisated by ionization source and entered to the mass analyser part. The main function of the mass analyzer is to separate, or resolve, the ions according to their mass-to-charge (m/z) ratios. There are a number of mass analysers with different features, including the m/z range that can be covered; the mass accuracy, and the achievable resolution are available. Tandem (MS-MS) mass spectrometers are instruments that have more than one analysers to have better resolution in analyzing the samples (Eberl, Mann et al.).

To define the effect of the absence of *Jmjd3* on the level of histone methylation, we used two different cell types; MEFs and foetal liver-derived macrophages obtained from E14.5 embryos for LC/MS-MS (mass spectrometry) analysis. The analysis was performed three times (three technical replicates) for both wildtype and the Knockout MEFs (Figure 22). Altogether, the mass spectrometry data identified the K4, K9, K27, and K79 methyl marks.

For K27 mark, around 5 times difference was observed in the case of dimethylated peptides (Figure 23) which could not be confirmed later at the protein level measuring by western blot analysis (Figure 28) which could be due to the less sensivity of the western blotting analysis compare to the mass spectrometry analysis.

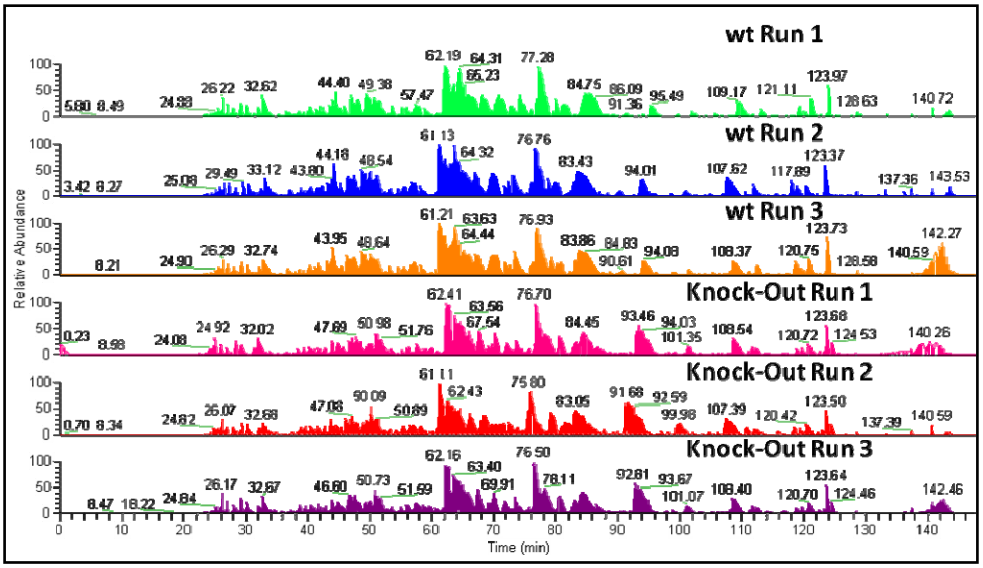

Figure 22. Total ion chromatogram (TIC) in triplicate relative to the Arg-C digestion of core histones purified from Jmjd3 wildtype and Knockout MEFs.

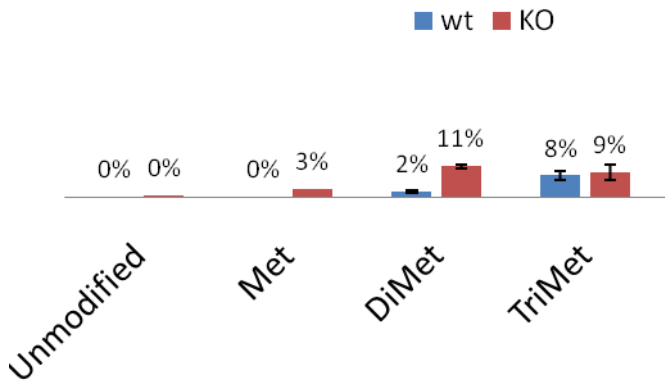

Figure 23. Relative quantification of H3K27 residue methyl marks in Jmjd3 wildtype versus knockout MEFs. A significant increase for the level of K27me2 was observed in jmjd3 KO MEFs compare to Wt MEFs (2% in Wt versus 11% in KO cells).

The K4, K9 and K79 methylated residues were detected by Mass spectrometry analysis. No significant differences were seen for these methylated marks in wildtype and knockout MEFs (Figure 24).

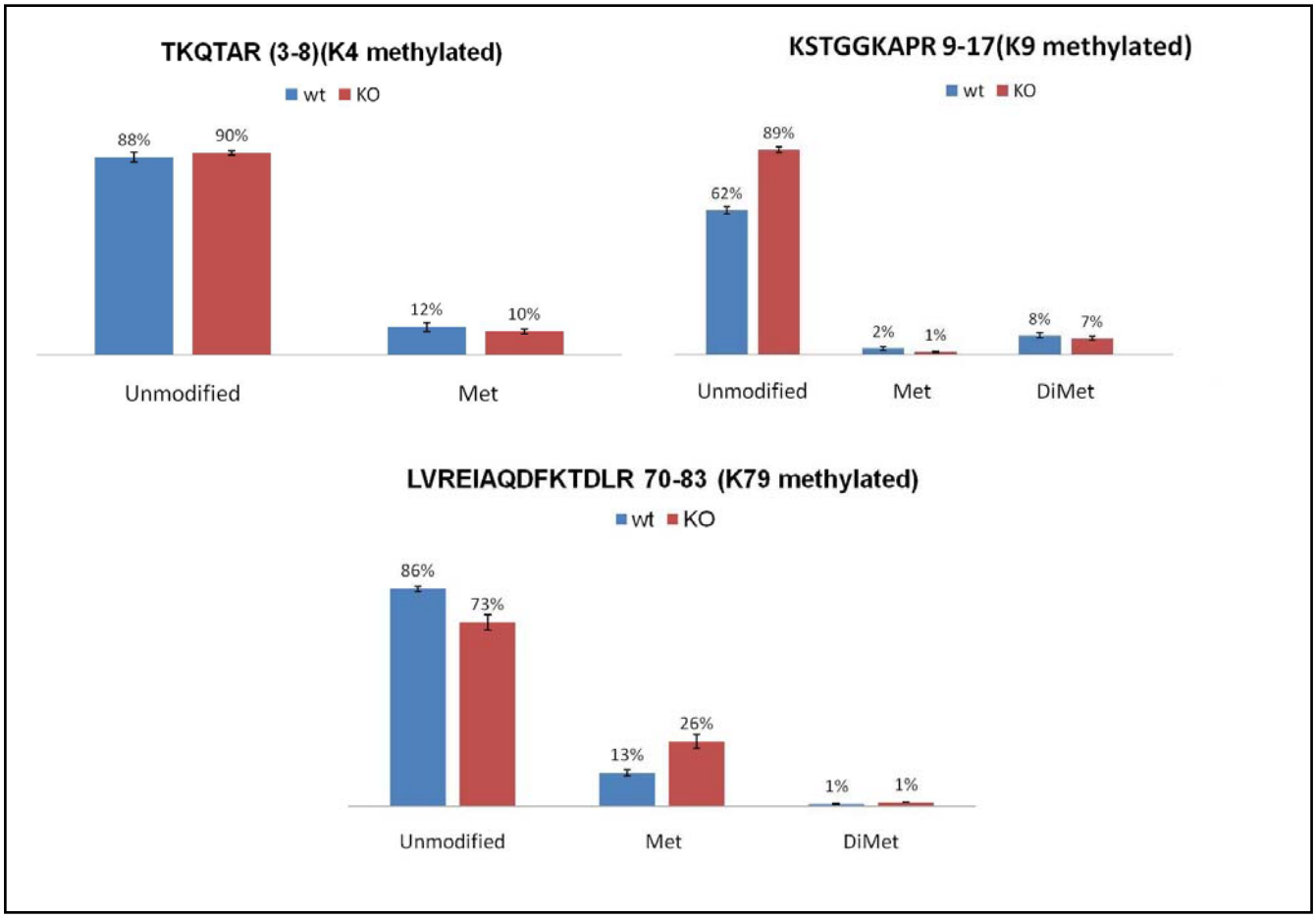

Figure 24. Relative quantification of methylation marks for K4, K9 and K79 residues of histone H3 in Jmjd3 wildtype versus knockout MEFs. The methylation changes were not significant for these residues.

LC/MSMS analysis was performed in triplicate (three independent runs) for wt, wt+LPS and *Jmjd3* Knockout+LPS foetal liver-derived macrophages (Figure 25).

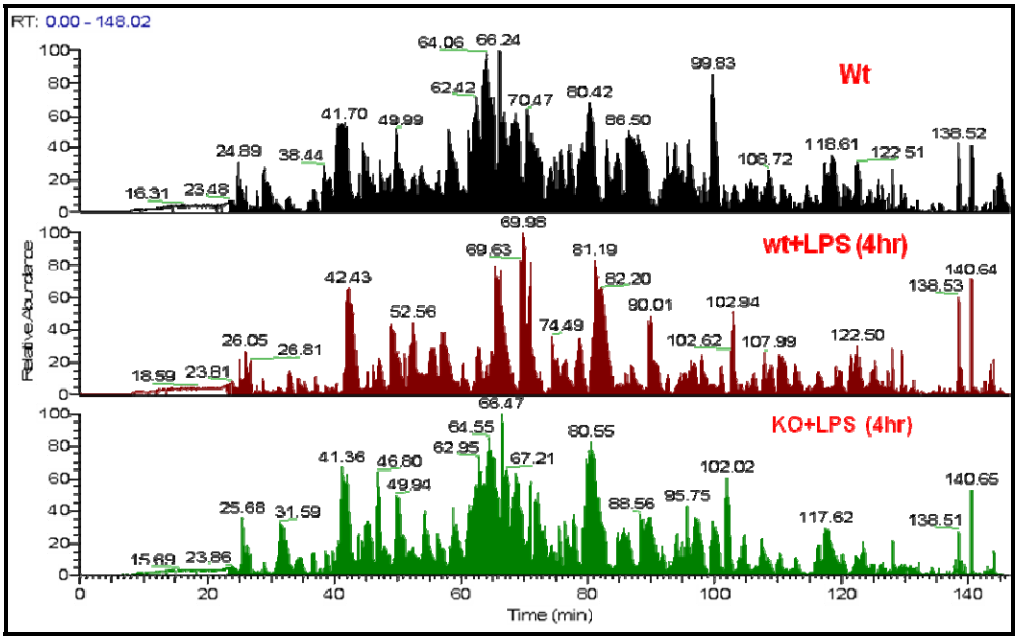

Figure 25. Total ion chromatogram (TIC) in triplicate relative to the Arg-C digestion of core histones purified from Jmjd3 wildtype and Knockout macrophages.

Altogether the mass spectrometry data allowed us to identify the K4, K9,K27,and K79 methyl marks on histone H3 and also the K20 on histone H4. The relative abundance for each species was estimated and the average values were obtained by the three technical replicates. The relative standard deviations were also calculated.

For K27 mark, the **K**SAPATGGVKKPHR peptide was identified as mono, di and three methylated. Considering the initial hypothesis that Jmjd3 is a histone demethylase for H3K27me3 mark and upregulated in response to LPS treatment in macrophages, we expected to see less K27me3 mark in wt macrophages treated with LPS and no decrease in H3K27me3 mark for Jmjd3 ko macrophages. This was actually the case, the relative abundance of K27me3 in wt macrophages untreated with LPS and the ko macrophages treated with LPS was equal showing that in macrophages, Jmjd3 is demethylating H3K27me3. However this result could not be confirmed by western blotting (Figure 28).

For K9 mark, a gain of relative abundance of me3 in the KO+LPS sample was measured in comparison to wt+ LPS. However, this K9 me3-KO level is NOT returning exactly to the level

in the wt sample, but actually is “bigger”(6% for the KO+LPS versus the 2% wt). Correspondingly, for the K9me2, a reduction was seen in the KO+LPS as compared to wt+LPS, but the decrease is more pronounced than in the wt.

As for K9 methylation pattern, It is also worth mentioning that the percentage of me3 in all the three states analyzed (wt, wt+LPS and KO+LPS macrophages) is always much lower than the one we usually observed for the same methyl-state in other cell lines (eg. HeLa or MEFs). In particular, here we “measured” a percentage of K9me3 ranging from 1-6% (the latter detected in the KO), while we usually observed about 10-15% of the same PTM.

We also reported the H3-K4, K79 and H4-K20 residues methylated. In these latest cases, variations were quite low (Figure 26).

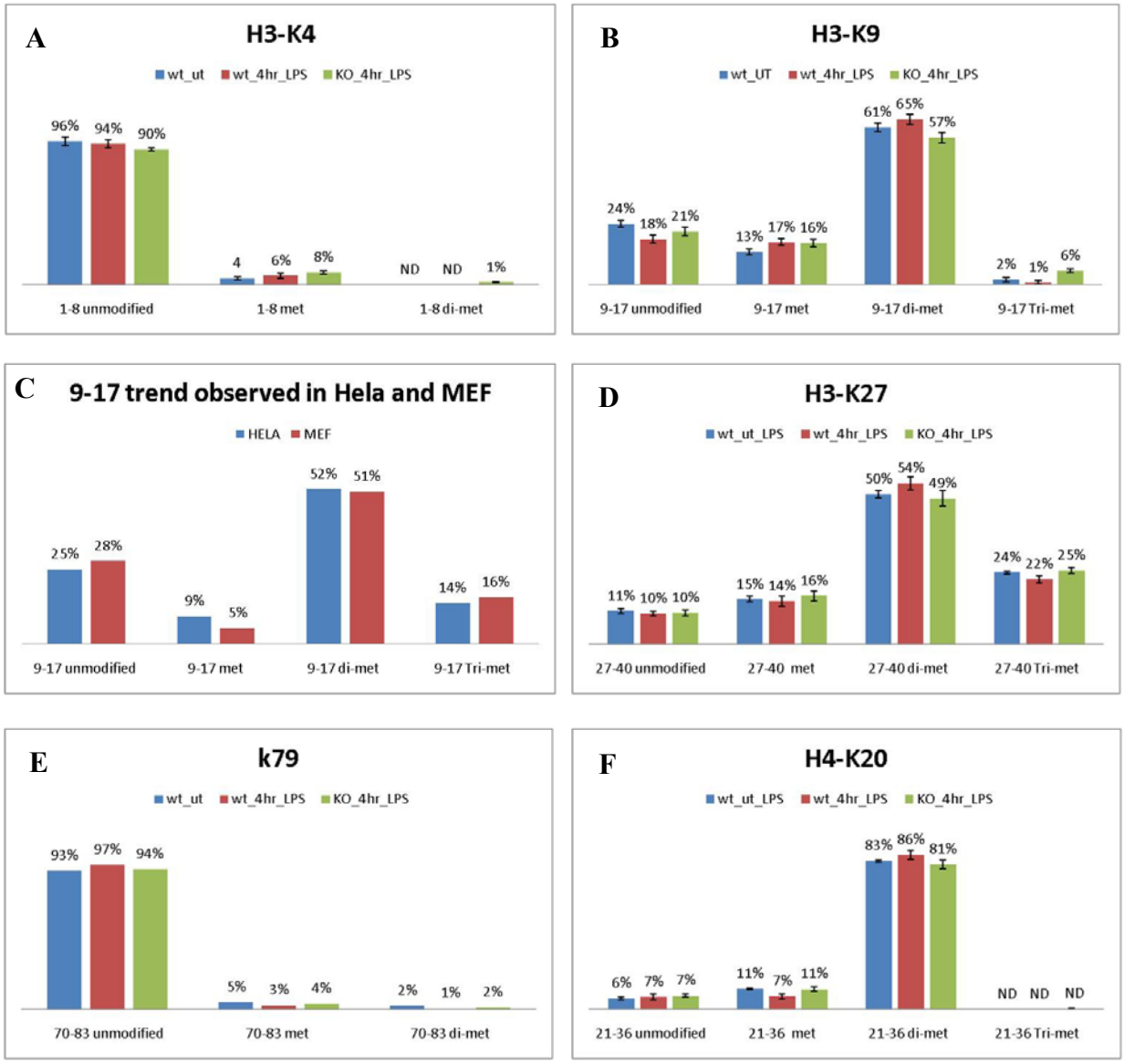

Figure 26. Mass Relative quantification of methylation marks for (A) K4, (B)K9, (D)K27 and (E)K79 residues of histone H3 and (F)K20 of histone H4 in Jmjd3 wildtype versus knockout macrophages. (C)K9 mass spectrometry analysis in Jmjd3 wildtype versus knockout MEFs. The methylation changes were not significant for these residues.

3. *Jmjd3* contribution to the transcriptional program of activated macrophages

To define the functional role of *Jmjd3* in the inflammatory response, we differentiated knock-out fetal liver cells derived from 14.5 dpc embryos towards macrophages. Macrophages obtained from these mice lacked Jmjd3 mRNA and protein (Figure 27).

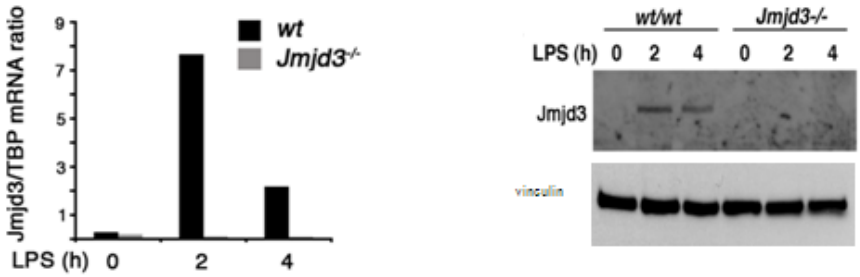

Figure 27. mRNA and protein level in *Jmjd3*$^{-/-}$ macrophages - *Jmjd3* expression at mRNA and protein level is abrogated in fetal liver-derived macrophages.

Macrophage differentiation and responsiveness to LPS activation was unperturbed, as indicated by the macrophage markers tested by FACs analyses, suggesting that Jmjd3 ablation does not influence macrophage development (Figure 28).

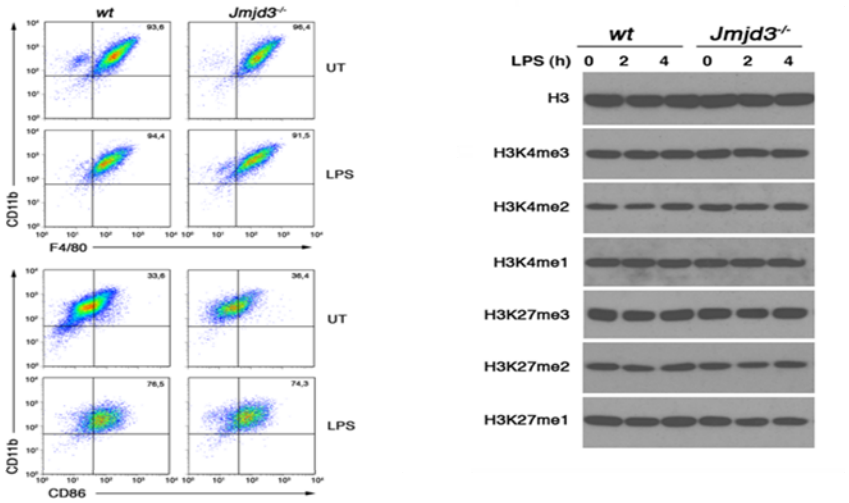

Figure 28. Analysis of histone methylation and differentiation in *Jmjd3*$^{-/-}$ macrophages. Macrophages derived from the fetal livers of Jmjd3$^{-/-}$ mice were analyzed for histone methylation at H3K4 and H3K27 (*a*). Differentiation markers (CD11b & F 4/80) and activation marker (CD86) in Jmjd3$^{-/-}$ macrophages are shown in (*b*).

The only known substrate of Jmjd3 is H3K27me3, and the simplest prediction consistent with its reported biochemical activity as a H3K27 demethylase is that Jmjd3 is recruited to genes associated with basal H3K27me3 levels in order to reduce them and enable or enhance transcriptional activation. To test this possibility, we analyzed the bulk levels of H3K27me3/2/1 and H3K4me3/2/1 in Jmjd3$^{-/-}$ cells. Western blot analysis showed that the bulk levels of H3K27me3/2/1 and H3K4me3/2/1 were not grossly affected by the absence of Jmjd3 (Figure 28). This result was supported by the ChIP-seq data on H3K27me3 in unstimulated and LPS-stimulated macrophages done by Francesca De Santa in our group. These data showed that Jmjd3 target genes in the majority of cases was not associated with any H3K27me3 peak within ± 1kb showing that in this system, H3K27me3 could not be considered as the substrate for Jmjd3.

Microarray analyses were performed from biological triplicates of LPS+IFNγ-treated (4h) wt or Jmjd3$^{-/-}$ fetal liver-derived macrophages. Using as cutoff a fold-change of 2, only 33

Threshold	Nr. of genes	Jmjd3 positive genes (%)
FC 2	33	14,7% (FDR 0,001) 20,5% (FDR 0,05)
FC 1,5	237	8,3% (FDR 0,001) 17,9% (FDR 0,05)
FC 1,4	478	5,4% (FDR 0,001) 14,01 % (FDR 0,05)

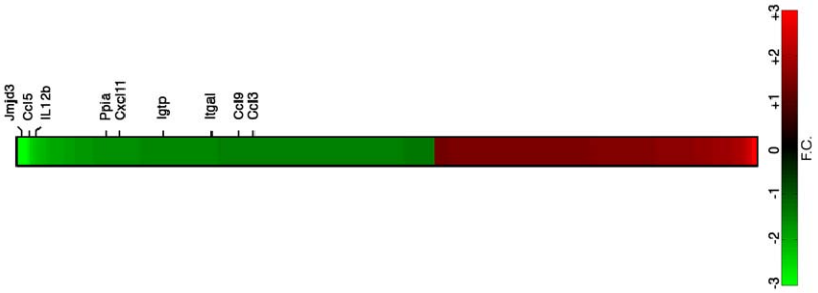

Figure 29. *Jmjd3* contribution to gene expression in LPS-activated macrophages. Summary of the microarray results, indicating the number of genes that are differentially expressed in wt vs. Jmjd3$^{-/-}$ macrophages at various thresholds and their binding to Jmjd3.

genes were differentially expressed in Jmjd3$^{-/-}$ cells, of which 20,5% were direct Jmjd3 targets. Considering a fold-change of 1.5 the expression of 237 genes was affected, while 478 genes were influenced by Jmjd3 deletion when a threshold of 1.4 was applied (Figure 29). The percentage of direct Jmjd3 targets, as evaluated by ChIP-Seq experiments using an anti-Jmjd3 antibody remained comparable at all thresholds.

Overall, the fact that the reduction in the selected threshold resulted in large increases in the amount of affected genes, while the percentage of direct *Jmjd3* targets remained comparable suggests that at most genes only small transcriptional effects are brought about by *Jmjd3*, consistent with the idea that similarly to other transcriptional coregulators of the JmjC family,

Jmjd3 tunes the transcriptional output without being absolutely necessary for the expression of any gene.

4. Response of *Jmjd3*$^{-/-}$ macrophages to bacterial infection

To define the consequences of *Jmjd3* ablation in the response to bacterial infection, we used *in vitro* and *in vivo* models.

4.1. Intracellular survival of Salmonella typhimurium is the same in macrophages from wild-type and *Jmjd*$^{-/-}$ mice in an *in vitro* assay.

To define the possible role of Jmjd3 in macrophage responses to bacterial infection, we set out an experiments according the protocol explained in section7 of methods and materials.

No difference in survival was found in the killing of Salmonella in different time points (4H, 8H and 24H). The initial recovery of intracellular bacteria at 2H which is considered as T0 was the same for both wildtype and *Jmjd3*$^{-/-}$ macrophages. Therefore, macrophages from *Jmjd3*$^{-/-}$ mice are not inherently different in their capacity to kill *Salmonella* compared with wildtype-derived macrophages (Figure 30).

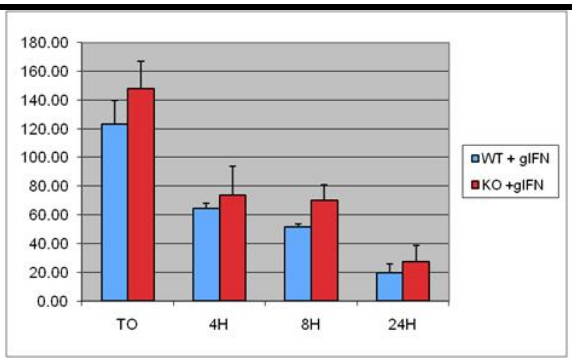

Figure 30 . Gentamicin take-up assay in fetal liver-derived macrophages. Significant difference in engulfed-salmonella survival was not found for different time points (4H, 8H and 24H).

Overall, variability among the experiments did not allow detecting any obvious and significant difference between the wt and ko macrophages in terms of bacterial killing.

4.2. Consequences of salmonella infection on *Jmjd*$^{-/-}$ *haematopoietic chimeras*

We set out to generate *haematopoietic* chimeras in order to have a model carrying the genetic mutation restricted to cells of the haematopoietic system and to define the effect of the Jmjd3 absence in the *haematopoietic* system. (Details in section 8; Methods & Materials)

At first the efficiency of reconstitution was assessed by FACS analysis. We got quit high percentage of reconstitution for the haematopoietic cells coming from C57Bl/6 donor mice transplanted into C57Bl/6 Ly5.1 recipients (Figure 31).

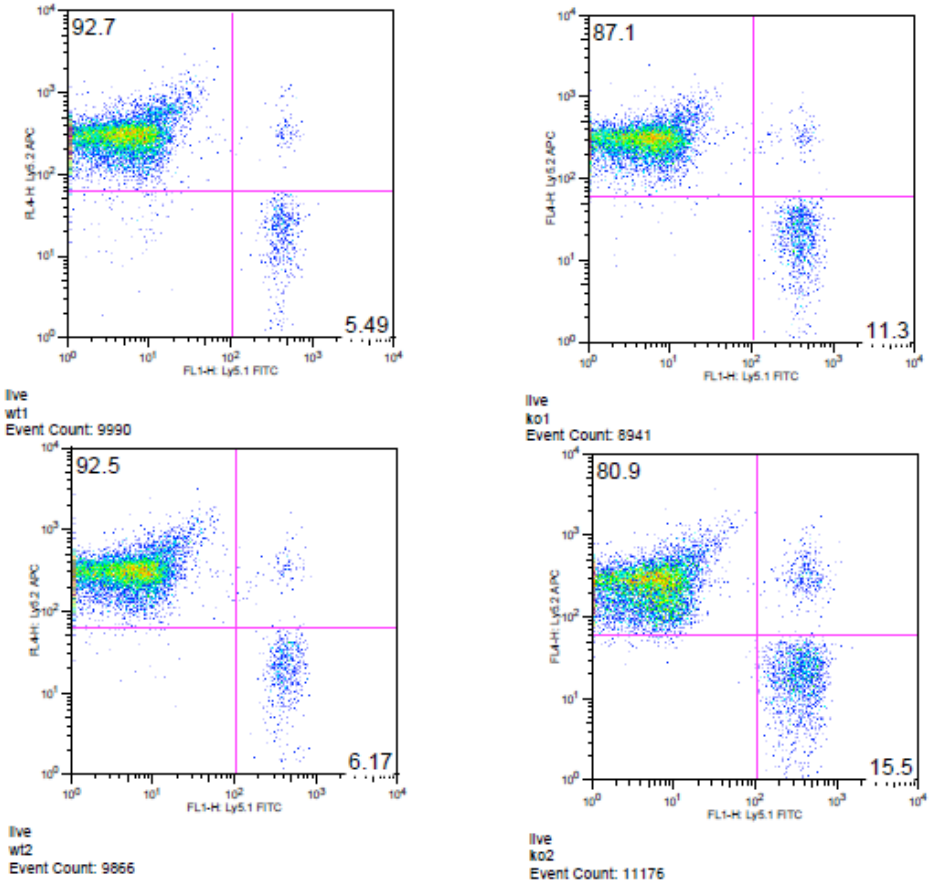

Figure 31 . FACS analysis for reconstituted mice using anti-Ly5.1 and anti-Ly5.2 antibodies. We had an efficient percentage of reconstitution (~80-90%) for the haematopoietic cells coming from C57Bl/6 donor mice transplanted into C57Bl/6 Ly5.1 recipients.

Reconstituted mice were infected with salmonella by oral gavage and sacrificed 5 days post infection. Bacterial loads were determined for liver, spleen, mesenteric lymph nodes (MLNs) and *Peyer's patches* in *Jmjd3*$^{-/-}$ and *Jmjd3*$^{+/+}$ reconstituted mice .

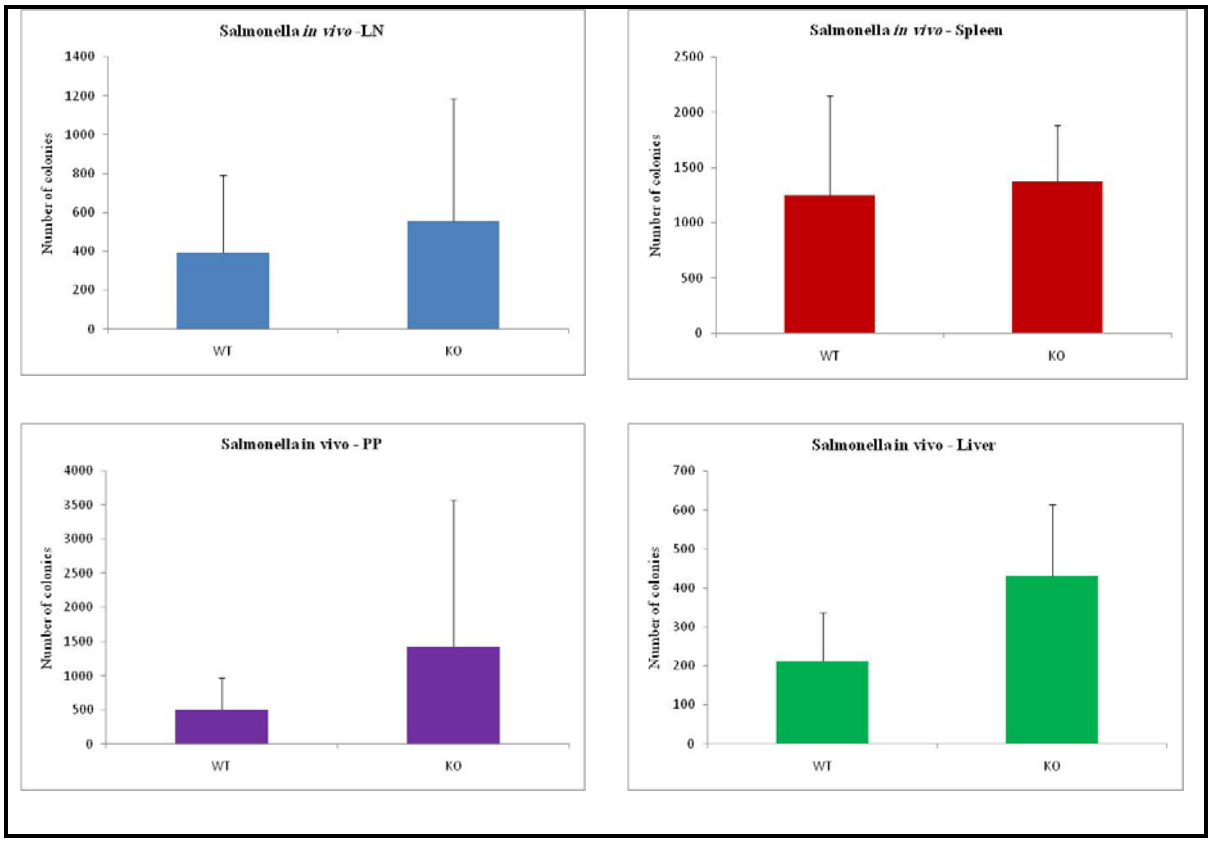

Figure 32 . The tissue colonization of mice inoculated with 5×10^6 wild-type *Salmonella* was determined 5 days after inoculation. No significant difference was found in response to infection in mutant mice comparing to the wildtypes.

Considering the big error bars in the experiment, we concluded that there is not a significant difference in the response to salmonella infection in Jmjd3 wildtype and knockout mice. To confirm the result of the last experiment, still I am trying to reconstitute more *Jmjd*$^{-/-}$ *haematopoietic chimeras* and repeat the test for more biological samples.

DISCUSSION

Perinatal lethality in Jmjd3$^{-/-}$ mice

In this study, we have generated mice lacking the histone demethylase; Jmjd3. These mice die within 24 hours of birth with severe respiratory failure. While some of the null mice had less activity, most appear normal at birth but then they start to breathe abnormally and die because of this problem. Thus, despite the wide distribution of Jmjd3 expression by most of the tissues and cell types (Figure 13), the abnormalities in the Jmjd3$^{-/-}$ mice were largely confined to the respiration control center in brainstem.

Since the discovery of histone demethylases in 2004, researchers tried to define the role of this group of enzyme in *in vitro* assays. More recently, model organisms have been used to define the roles of demethylases *in vivo*. For example, KDM7, a JmjC domain-containing protein, catalyzes demethylation of both mono- and dimethylated H3K9 and H3K27. Inhibition of KDM7 orthologs in zebrafish resulted in developmental brain defects {Tsukada, 2010 #131}. KDM7 belongs to the subfamily of JmjC proteins composed of PHF2 and PHF8. *Phf2* is expressed predominantly in the embryonic neural tube and root ganglia in mice, and mutation of PHF8 in human causes inherited X-linked mental retardation (Laumonnier, Holbert et al. 2005). KDM5C (formerly SMCX/JARID1C) is H3K4me3 demethylase contains the catalytic JmjC domain. Inhibition of kdm5c in zebrafish resulted in significant defects in neuronal development, including increased neuronal cell death. Moreover, kdm5c inhibition in primary mammalian neurons impaired dendritic morphogenesis (Iwase, Lan et al. 2007). Knockout mice for RBP2, a H3K4 demethylase, appear to be grossly normal and just have a mild hematological abnormalities, including increased cell cycling and enhanced survival of myeloid progenitor cells (Klose, Yan et al. 2007).KDM6A (formerly UTX) is a histone H3K27 demethylase which is expressed in the neuroectoderm of the brain and neural tube at E9.5 in mouse embryo. Kdm6a mutant embryos showed exencephaly in the mid-and hindbrain region. Histological sections through the head in these mutants showed that the forebrain

vesicle fails to fuse in the rostral region and the optic pits are asymmetrical in the mutant embryos (Cox, Vollmer et al.). Absence of KDM1A (formerly LSD1/*Aof2*) in mouse causes embryonic lethality. In this model, embryonic development is arrested at or before E5.5, the egg cylinder failed to elongate and undergo gastrulation and embryos are resorbed by E7.5. KDM1A deficiency in ES cells results in growth and differentiation defects due to increased cell death and impaired cell cycle progression (Wang, Hevi et al. 2009). Disruption of KDM1B, a H3K4me2/me1 demethylase, had no effect on mouse development and oogenesis. However, oocytes from KDM1B-deficient females showed an increase in the level of H3K4 methylation and failed to establish DNA methylation imprints at multiple loci. Therefore, embryos derived from these oocytes had biallelic expression or suppression for some genes and died before mid-gestation (Ciccone, Su et al. 2009). Male mice that lack JHDM2A/KDM3A are viable but infertile, with smaller testes and severe defects in spermatogenesis. The obese phenotype is also observed in JHDM2A knockout mice due to defects in the expression of metabolic genes and impairs β-oxidation and glycerol release in skeletal muscle (Okada, Scott et al. 2007; Tateishi, Okada et al. 2009). All Jarid2 (formerly Jumonji) knockout mouse embryos died before embryonic day 15.5. Some of the homozygotes developed an abnormal groove in a region just anterior to the midbrain-hindbrain boundary on the neural plate at embryonic day 8-8.5 and showed a defect in neural tube closure in the midbrain region (Takeuchi, Yamazaki et al. 1995). The JMJD6 mutant has transient developmental defects during mid fetal development. The mutant embryos exhibits massive subcutaneous edema compared to a wild type (Bose, Gruber et al. 2004; Schneider, Bose et al. 2004). Some research showed the role of some of the demethylases in meiosis. For example, in S. pombe, LSD1/KDM1 functions as an H3K9me2/1 demethylase, and the ablation of this demethylase results in a sporulation defect (Lan, Zaratiegui et al. 2007).

This type of studies suggested that histone demethylases for H3K27me have function later in differentiation and development. For example, a role for H3K27me3 demethylation in mammalian neuronal development has been identified. They showed that H3K27me3 demethylation is crucial for mouse forebrain development (Jepsen, Solum et al. 2007).

The defect which has been seen in the Jmjd3$^{-/-}$ mouse model in this study is due to the failure of the preBötC to generate a rhythmic respiratory drive. The ability to produce rhythmic motor behaviors linked to respiratory function is a property of the brainstem reticular formation, which has been remarkably conserved during the evolution of vertebrates. There are conservative developmental mechanisms orchestrating the organogenesis of the brainstem. In vertebrates, the hindbrain is one of the vesicles that appear at the anterior end of the neural tube of the embryo. Further morphogenetic subdivision ensues whereby the hindbrain neuroepithelium becomes partitioned into an iterated series of compartments called rhombomeres. The segmentation process is believed to determine neuronal fates by encoding positional information along the rostro-caudal axis. Before and at the onset of segmentation, genes encoding transcription factors such as *Hox*, *Krox-20*, *kreisler*, are expressed in domains corresponding to the limits of future rhombomeres. Inactivation of these genes specifically disturbs the rhombomeric pattern of the hindbrain. It supposed that this primordial rhombomeric organisation influences later function of respiratory control networks in chicks and mice.

Experiments which were performed in embryos and after birth in transgenic mice have been shown that although expression of developmental genes and hindbrain segmentation are transient events of early embryonic development, they are important for the process of respiratory rhythm generation by brainstem neuronal networks. Furthermore, *in vivo* and *in vitro* analysis of neurons in transgenic mice revealed postnatal respiratory phenotypes associated with defects of central pontine and/or afferent respiratory control in *Krox-20*,

Hoxa1 and *kreisler* mutants. Altogether, these experiments indicate that segmentation-related specifications of the hindbrain rhythmic neuronal network influences the respiratory patterns after birth (Champagnat and Fortin 1997; del Toro, Borday et al. 2001; Chatonnet, Borday et al. 2006). As H3K27me3 mark is one of the post-translational modification which has been shown that has a transcriptional regulation role in the expression of Hox genes and Jmjd3 is the demethylase enzyme which can demethylate this mark, the respiratory phenotype defect which has been seen in Jmjd3 knockout can be explained in this context.

Jmjd3-mediated transcriptional control in LPS-activated macrophages

In this study and the parallel study in our lab, we tried to define the role of Jmjd3 in the gene expression program of LPS-activated mouse macrophages. Combining the data obtained by analyses of hypomorph jmjd3 $^{-/-}$ mice and ChIP-sequencing data obtained by francesca De santa in our lab led us to conclude the following:

(i) Jmjd3 is recruited to the TSSs of thousands of active and inducible genes in LPS-activated macrophages ; (ii) Recruitment correlates with H3K4me3 and Pol_II recruitment which is the representors of gene activity; (iii) No gene requires Jmjd3 for expression; (iv) Most Jmjd3 target genes are apparently not affected by Jmjd3 deletion; (v) a few hundred genes showed mild (less than two-fold) mRNA changes in the absence of Jmjd3; (vi) a few (biologically relevant) genes (e.g. IL12b, Ccl5) are more dependent on Jmjd3 for optimal transcriptional activity; (vii) no gene was completely dependent on Jmjd3 for induction or expression; (ix) Jmjd3 effects seem to be largely independent of H3K27me3 demethylation. Our finding in this study which shows that the absence of Jmjd3 has a mild effect (less than two-fold) on the inflammatory transcription machinery is quite common to several transcriptional coregulators (paticulary histone-modifying enzymes). For example, transcriptional profiling experiments (Miller, Krogan et al. 2001; Bernstein, Humphrey et al.

2002) have identified genes whose expression appears to be affected by the loss of Set1, and basically the effects were quantitatively modest. In these experiments, they showed that the deletion of Set1 (the only H3K4 histone methyltransferase in the genome of *Saccharomyces cerevisiae*) caused very limited effects on transcription, with only 20 genes affected by more than 1.5-fold, in spite of its widespread association with the TSS of active genes (Ng, Robert et al. 2003) .

This scenario has been seen for Menin which is a component of a subset of MLL complexes. This 67-kDa protein is broadly associated with the TSSs of active genes and functions as a general transcriptional regulator that helps maintain stable gene expression. Contrary to what one predict given the broad range of promoters targeted by menin, no significant differences in the expression of menin-targeted genes were seen in menin-null cells compared to wild type (Scacheri, Davis et al. 2006). Depletion of Ash2L, a component of the MLL and SET complex, also showed a mild reduction in the efficiency of pre-mRNA splicing (~3-fold) without any detectable impact on Pol_II recruitment and transcript levels (Sims, Millhouse et al. 2007)

The same behaviour was reported for PcG proteins, which are broadly associated with silent or repressed genes. For example, Ezh2 ablation in human fibroblasts caused ~ 1.2 fold expression change in about 350 genes, of which 10% were the direct targets of Ezh2. This depletion did not have any marginally effect on the transcriptional level of 1000 genes bound by Ezh2 (Bracken, Dietrich et al. 2006).

Apart from this kind of behavior of several coregulators to bring about small transcriptional changes, in the specific system an additional factor which is likely contributes to reduce the extent of detectable effects of coregulator depletion is mRNA stabilization (Anderson 2009). Many of the 3' untranslated regions of short-lived mRNAs have adenine- and uridine-ich destabilizing elements (AREs) that promotes mRNA decay. This AREs content can be a part

of regulatory mechanism in inflammatory response and has the potency to mask the effect of the depletion of transcription coregulator (Anderson 2008; Hao and Baltimore 2009).

Given the mentioned premises, It is tempting to speculate that in analogy to other coregulators, Jmjd3 may have a final impact on the system that reflects the combination of a fairly large amount of simultaneous small changes, rather than a limited number of effects of high intensity (like those observed with several sequence-specific transcription factors). A similar concept is true for the biological effects of microRNAs, which in most cases change mRNA and protein levels of dozens or hundreds of targets by no more than 10–20% (Baek, Villen et al. 2008).

Although the absence of Jmjd3 has a modest effect (less than two-fold) on most of the inflammatory genes, a few genes are affected quite high by this ablation. Ccl5 and IL12b which mediate recruitment and Th1 polarization of T lymphocytes are the ones which shows high dependency on Jmjd3. Overall, the list of genes whose expression is directly or indirectly affected by Jmjd3 deletion includes several known players of the inflammatory and immune response such as chemokines (Ccl3, Ccl4, Ccl5, Ccl9, Cxcl11), cytokines (e. g. Il12b, Il6) and antimicrobial molecules (e. g. the GTPase Igtp).

More studies focusing on the in vivo aspects of Jmjd3 biology in in vivo models will allow us to gain a better understanding of this molecular regulator of gene expression (De Santa, Narang et al. 2009).

Activated macrophages have a stable H3K27me3 mark

Although it has recently been demonstrated that histone lysine methylation can be dynamically regulated by new indentified histone demethylases (Shi, Lan et al. 2004; Tsukada, Fang et al. 2006), but in fact the global histone methylation turnover is relatively low(Byvoet, Shepherd et al. 1972; Duerre and Lee 1974).

Around 30 JmjC domain-containing proteins have been identified in mammals. For some of them, methylated lysine in histone tail is already identified as the relevant substrate. And the depletion of these enzymes has an effect on the methylation level of the histones. However, the possibility that non-histone substrates or non-enzymatic activities (such as structural functions in multi-molecular complexes) of histone demethylases may mediate the biological roles of these enzymes is also emerging in this context (Huang and Berger 2008). For example, LSD1 can demethylate the tumor suppressor p53 (Huang, Sengupta et al. 2007). It is clear that assumption that histones are the only substrates on which the JmjC proteins act is completely incorrect.

Overall, our data show no global reductions in H3K27me3 levels when Jmjd3 is removed in fetal liver-derived macrophages. The same scenario exist for JARID2 when JARID2 is removed in ES cells, the global reductions in histone methyl marks have not been seen. Regarding JARID2, it has been shown that knockdown of JARID2 results in increased H3K27me3 levels on some target genes and decreased H3K27me3 on others. The observed increase in H3K27me3 levels on some PRC2 target genes and the reduction of H3K27me3 on others upon JARID2 knockdown could cancel each other out in the measurement of bulk H3K27 methylation levels, the same scenario could be right in case of Jmjd3 knockout. Since we do not have any direct evidence showing that Jmjd3 demethylate H3K27me3 in the early window of time, we can suggest that the early transcriptional program occurring in the first hours after microbial stimulation is independent of H3K27me3 demethylation, although more data are required to confirm this possibility. Moreover, the genes most affected by Jmjd3 deletion (e.g. Ccl5) are H3K27me3 negative and do not show any increase in H3K27me3 in Jmjd3 KO cells.

Whether the enzymatic activity of Jmjd3 is required in controlling the inflammatory gene expression is still an open question that remains to be addressed using proper approaches.

Our study shows that jmjd3 is crucial for mouse brainstem development. The defect in jmjd3$^{-/-}$ mouse is due to the failure of neural development in the PreBötC complex located at the respiratory area in the brainstem which is generating a rhythmic respiratory derive. The knockout mouse has perinatal lethality due to the respiration failure which is caused by the mentioned defect at the respiratory area in the brainstem. Besides the role in development and tissue renewal, *Jmjd3* participates in the inflammatory transcriptional response induced by LPS stimulation in macrophages.

Overall, Jmjd3 effects on the inflammatory transcriptional output is not widespread and also is not histone-demethylase independent manner but in most cases its main role is to fine tune the transcription rates of several genes in inflammatory response.

BIBLIOGRAPHY

Agger, K., P. A. Cloos, et al. (2007). "UTX and JMJD3 are histone H3K27 demethylases involved in HOX gene regulation and development." Nature **449**(7163): 731-4.

Agger, K., P. A. Cloos, et al. (2009). "The H3K27me3 demethylase JMJD3 contributes to the activation of the INK4A-ARF locus in response to oncogene- and stress-induced senescence." Genes Dev **23**(10): 1171-6.

Allfrey, V. G., R. Faulkner, et al. (1964). "Acetylation and Methylation of Histones and Their Possible Role in the Regulation of Rna Synthesis." Proc Natl Acad Sci U S A **51**: 786-94.
Anderson, P. (2008). "Post-transcriptional control of cytokine production." Nat Immunol **9**(4): 353-9.

Anderson, P. (2009). "Intrinsic mRNA stability helps compose the inflammatory symphony." Nat Immunol **10**(3): 233-4.

Baek, D., J. Villen, et al. (2008). "The impact of microRNAs on protein output." Nature **455**(7209): 64-71.

Bannister, A. J. and T. Kouzarides (2005). "Reversing histone methylation." Nature **436**(7054): 1103-6.

Bannister, A. J., R. Schneider, et al. (2002). "Histone methylation: dynamic or static?" Cell **109**(7): 801-6.

Bannister, A. J., P. Zegerman, et al. (2001). "Selective recognition of methylated lysine 9 on histone H3 by the HP1 chromo domain." Nature **410**(6824): 120-4.

Barradas, M., E. Anderton, et al. (2009). "Histone demethylase JMJD3 contributes to epigenetic control of INK4a/ARF by oncogenic RAS." Genes Dev **23**(10): 1177-82.

Berger, S. L. (2007). "The complex language of chromatin regulation during transcription." Nature **447**(7143): 407-12.

Bernstein, B. E., E. L. Humphrey, et al. (2002). "Methylation of histone H3 Lys 4 in coding regions of active genes." Proc Natl Acad Sci U S A **99**(13): 8695-700.

Binda, C., A. Mattevi, et al. (2002). "Structure-function relationships in flavoenzyme-dependent amine oxidations: a comparison of polyamine oxidase and monoamine oxidase." J Biol Chem **277**(27): 23973-6.

Bonenfant, D., H. Towbin, et al. (2007). "Analysis of dynamic changes in post-translational modifications of human histones during cell cycle by mass spectrometry." Mol Cell Proteomics **6**(11): 1917-32.

Bose, J., A. D. Gruber, et al. (2004). "The phosphatidylserine receptor has essential functions during embryogenesis but not in apoptotic cell removal." J Biol **3**(4): 15.

Bracken, A. P., N. Dietrich, et al. (2006). "Genome-wide mapping of Polycomb target genes unravels their roles in cell fate transitions." Genes Dev **20**(9): 1123-36.
Bracken, A. P., D. Kleine-Kohlbrecher, et al. (2007). "The Polycomb group proteins bind throughout the INK4A-ARF locus and are disassociated in senescent cells." Genes Dev **21**(5): 525-30.

Burgold, T., F. Spreafico, et al. (2008). "The histone H3 lysine 27-specific demethylase Jmjd3 is required for neural commitment." PLoS One **3**(8): e3034.

Byvoet, P., G. R. Shepherd, et al. (1972). "The distribution and turnover of labeled methyl groups in histone fractions of cultured mammalian cells." Arch Biochem Biophys **148**(2): 558-67.

Cedar, H. and Y. Bergman (2009). "Linking DNA methylation and histone modification: patterns and paradigms." Nat Rev Genet **10**(5): 295-304.

Champagnat, J. and G. Fortin (1997). "Primordial respiratory-like rhythm generation in the vertebrate embryo." Trends Neurosci **20**(3): 119-24.

Chatonnet, F., C. Borday, et al. (2006). "Ontogeny of central rhythm generation in chicks and rodents." Respir Physiol Neurobiol **154**(1-2): 37-46.

Chen, Y., Y. Yang, et al. (2006). "Crystal structure of human histone lysine-specific demethylase 1 (LSD1)." Proc Natl Acad Sci U S A **103**(38): 13956-61.

Chen, Z., J. Zang, et al. (2007). "Structural basis of the recognition of a methylated histone tail by JMJD2A." Proc Natl Acad Sci U S A **104**(26): 10818-23.

Chinenov, Y. (2002). "A second catalytic domain in the Elp3 histone acetyltransferases: a candidate for histone demethylase activity?" Trends Biochem Sci **27**(3): 115-7.

Ciccone, D. N., H. Su, et al. (2009). "KDM1B is a histone H3K4 demethylase required to establish maternal genomic imprints." Nature **461**(7262): 415-8.

Cloos, P. A., J. Christensen, et al. (2006). "The putative oncogene GASC1 demethylates tri- and dimethylated lysine 9 on histone H3." Nature **442**(7100): 307-11.

Cox, B. J., M. Vollmer, et al. "Phenotypic annotation of the mouse X chromosome." Genome Res **20**(8): 1154-64.

Cuomo, A., S. Moretti, et al. (2010). "SILAC-based proteomic analysis to dissect the "histone modification signature" of human breast cancer cells." Amino Acids.

Dahle, O., A. Kumar, et al. "Nodal signaling recruits the histone demethylase Jmjd3 to counteract polycomb-mediated repression at target genes." Sci Signal **3**(127): ra48.

Dai, J. P., J. Y. Lu, et al. "Jmjd3 activates Mash1 gene in RA-induced neuronal differentiation of P19 cells." J Cell Biochem **110**(6): 1457-63.

De Santa, F., I. Barozzi, et al. (2010). "A large fraction of extragenic RNA pol II transcription sites overlap enhancers." PLoS Biol **8**(5): e1000384.
De Santa, F., V. Narang, et al. (2009). "Jmjd3 contributes to the control of gene expression in LPS-activated macrophages." Embo J **28**(21): 3341-52.

De Santa, F., M. G. Totaro, et al. (2007). "The histone H3 lysine-27 demethylase Jmjd3 links inflammation to inhibition of polycomb-mediated gene silencing." Cell **130**(6): 1083-94.

del Toro, E. D., V. Borday, et al. (2001). "Generation of a novel functional neuronal circuit in Hoxa1 mutant mice." J Neurosci **21**(15): 5637-42.

Dhalluin, C., J. E. Carlson, et al. (1999). "Structure and ligand of a histone acetyltransferase bromodomain." Nature **399**(6735): 491-6.

Di Stefano, L., J. Y. Ji, et al. (2007). "Mutation of Drosophila Lsd1 disrupts H3-K4 methylation, resulting in tissue-specific defects during development." Curr Biol **17**(9): 808-12.

Duerre, J. A. and C. T. Lee (1974). "In vivo methylation and turnover of rat brain histones." J Neurochem **23**(3): 541-7.

Eberl, H. C., M. Mann, et al. "Quantitative Proteomics for Epigenetics." Chembiochem.
Fischle, W., Y. Wang, et al. (2003). "Binary switches and modification cassettes in histone biology and beyond." Nature **425**(6957): 475-9.

Fodor, B. D., S. Kubicek, et al. (2006). "Jmjd2b antagonizes H3K9 trimethylation at pericentric heterochromatin in mammalian cells." Genes Dev **20**(12): 1557-62.

Gao, Y., P. Hyttel, et al. "Regulation of H3K27me3 and H3K4me3 during early porcine embryonic development." Mol Reprod Dev **77**(6): 540-9.

Garcia, B. A., C. M. Barber, et al. (2005). "Modifications of human histone H3 variants during mitosis." Biochemistry **44**(39): 13202-13.

Ghisletti, S., I. Barozzi, et al. "Identification and characterization of enhancers controlling the inflammatory gene expression program in macrophages." Immunity **32**(3): 317-28.

Godmann, M., V. Auger, et al. (2007). "Dynamic regulation of histone H3 methylation at lysine 4 in mammalian spermatogenesis." Biol Reprod **77**(5): 754-64.

Gray, S. G. and T. J. Ekstrom (2001). "The human histone deacetylase family." Exp Cell Res **262**(2): 75-83.

Gregoretti, I. V., Y. M. Lee, et al. (2004). "Molecular evolution of the histone deacetylase family: functional implications of phylogenetic analysis." J Mol Biol **338**(1): 17-31.

Hanson, R. W. and L. Reshef (1997). "Regulation of phosphoenolpyruvate carboxykinase (GTP) gene expression." Annu Rev Biochem **66**: 581-611.

Hanson, R. W. and L. Reshef (2003). "Glyceroneogenesis revisited." Biochimie **85**(12): 1199-205.
Hao, S. and D. Baltimore (2009). "The stability of mRNA influences the temporal order of the induction of genes encoding inflammatory molecules." Nat Immunol **10**(3): 281-8.

He, L., J. X. Yu, et al. (1998). "RIZ1, but not the alternative RIZ2 product of the same gene, is underexpressed in breast cancer, and forced RIZ1 expression causes G2-M cell cycle arrest and/or apoptosis." Cancer Res **58**(19): 4238-44.

Hebbes, T. R., A. W. Thorne, et al. (1988). "A direct link between core histone acetylation and transcriptionally active chromatin." Embo J **7**(5): 1395-402.

Ho, L. and G. R. Crabtree "Chromatin remodelling during development." Nature **463**(7280): 474-84.

Hong, S., Y. W. Cho, et al. (2007). "Identification of JmjC domain-containing UTX and JMJD3 as histone H3 lysine 27 demethylases." Proc Natl Acad Sci U S A **104**(47): 18439-44.

Huang, J. and S. L. Berger (2008). "The emerging field of dynamic lysine methylation of non-histone proteins." Curr Opin Genet Dev **18**(2): 152-8.

Huang, J., R. Sengupta, et al. (2007). "p53 is regulated by the lysine demethylase LSD1." Nature **449**(7158): 105-8.

Hublitz, P., M. Albert, et al. (2009). "Mechanisms of transcriptional repression by histone lysine methylation." Int J Dev Biol **53**(2-3): 335-54.

Hume, R., A. Burchell, et al. (2005). "Glucose homeostasis in the newborn." Early Hum Dev **81**(1): 95-101.

Ishii, M., H. Wen, et al. (2009). "Epigenetic regulation of the alternatively activated macrophage phenotype." Blood **114**(15): 3244-54.

Iwase, S., F. Lan, et al. (2007). "The X-linked mental retardation gene SMCX/JARID1C defines a family of histone H3 lysine 4 demethylases." Cell **128**(6): 1077-88.

Iyer, N. G., H. Ozdag, et al. (2004). "p300/CBP and cancer." Oncogene **23**(24): 4225-31.

Jepsen, K., D. Solum, et al. (2007). "SMRT-mediated repression of an H3K27 demethylase in progression from neural stem cell to neuron." Nature **450**(7168): 415-9.

Johansen, K. M. and J. Johansen (2006). "Regulation of chromatin structure by histone H3S10 phosphorylation." Chromosome Res **14**(4): 393-404.

Katz, D. J., T. M. Edwards, et al. (2009). "A C. elegans LSD1 demethylase contributes to germline immortality by reprogramming epigenetic memory." Cell **137**(2): 308-20.

Klose, R. J., E. M. Kallin, et al. (2006). "JmjC-domain-containing proteins and histone demethylation." Nat Rev Genet **7**(9): 715-27.

Klose, R. J., Q. Yan, et al. (2007). "The retinoblastoma binding protein RBP2 is an H3K4 demethylase." Cell **128**(5): 889-900.

Klose, R. J. and Y. Zhang (2007). "Regulation of histone methylation by demethylimination and demethylation." Nat Rev Mol Cell Biol **8**(4): 307-18.

Kouzarides, T. (2007). "Chromatin modifications and their function." Cell **128**(4): 693-705.
Lachner, M., D. O'Carroll, et al. (2001). "Methylation of histone H3 lysine 9 creates a binding site for HP1 proteins." Nature **410**(6824): 116-20.

Lan, F., P. E. Bayliss, et al. (2007). "A histone H3 lysine 27 demethylase regulates animal posterior development." Nature **449**(7163): 689-94.

Lan, F., M. Zaratiegui, et al. (2007). "S. pombe LSD1 homologs regulate heterochromatin propagation and euchromatic gene transcription." Mol Cell **26**(1): 89-101.

Laumonnier, F., S. Holbert, et al. (2005). "Mutations in PHF8 are associated with X linked mental retardation and cleft lip/cleft palate." J Med Genet **42**(10): 780-6.

Lee, D. Y., J. J. Hayes, et al. (1993). "A positive role for histone acetylation in transcription factor access to nucleosomal DNA." Cell **72**(1): 73-84.

Lee, J. S., E. Smith, et al. "The language of histone crosstalk." Cell **142**(5): 682-5.

Lee, M. G., R. Villa, et al. (2007). "Demethylation of H3K27 regulates polycomb recruitment and H2A ubiquitination." Science **318**(5849): 447-50.

Lee, M. G., C. Wynder, et al. (2006). "Functional interplay between histone demethylase and deacetylase enzymes." Mol Cell Biol **26**(17): 6395-402.

Leighton, P. A., K. J. Mitchell, et al. (2001). "Defining brain wiring patterns and mechanisms through gene trapping in mice." Nature **410**(6825): 174-9.

Loh, Y. H., W. Zhang, et al. (2007). "Jmjd1a and Jmjd2c histone H3 Lys 9 demethylases regulate self-renewal in embryonic stem cells." Genes Dev **21**(20): 2545-57.

Marks, P., R. A. Rifkind, et al. (2001). "Histone deacetylases and cancer: causes and therapies." Nat Rev Cancer **1**(3): 194-202.

Martin, C. and Y. Zhang (2005). "The diverse functions of histone lysine methylation." Nat Rev Mol Cell Biol **6**(11): 838-49.

Martinez-Balbas, M. A., U. M. Bauer, et al. (2000). "Regulation of E2F1 activity by acetylation." Embo J **19**(4): 662-71.

Maurer-Stroh, S., N. J. Dickens, et al. (2003). "The Tudor domain 'Royal Family': Tudor, plant Agenet, Chromo, PWWP and MBT domains." Trends Biochem Sci **28**(2): 69-74.

Miller, T., N. J. Krogan, et al. (2001). "COMPASS: a complex of proteins associated with a trithorax-related SET domain protein." Proc Natl Acad Sci U S A **98**(23): 12902-7.

Milne, T. A., S. D. Briggs, et al. (2002). "MLL targets SET domain methyltransferase activity to Hox gene promoters." Mol Cell **10**(5): 1107-17.

Mitchell, K. J., K. I. Pinson, et al. (2001). "Functional analysis of secreted and transmembrane proteins critical to mouse development." Nat Genet **28**(3): 241-9.

Mosammaparast, N. and Y. Shi (2010). "Reversal of histone methylation: biochemical and molecular mechanisms of histone demethylases." Annu Rev Biochem **79**: 155-79.

Mosser, D. M. and J. P. Edwards (2008). "Exploring the full spectrum of macrophage activation." Nat Rev Immunol **8**(12): 958-69.

Munshi, A., G. Shafi, et al. (2009). "Histone modifications dictate specific biological readouts." J Genet Genomics **36**(2): 75-88.

Nakamura, T., T. Mori, et al. (2002). "ALL-1 is a histone methyltransferase that assembles a supercomplex of proteins involved in transcriptional regulation." Mol Cell **10**(5): 1119-28.

Natoli, G. "Maintaining Cell Identity through Global Control of Genomic Organization." Immunity **33**(1): 12-24.

Natoli, G., G. Testa, et al. (2009). "The future therapeutic potential of histone demethylases: A critical analysis." Curr Opin Drug Discov Devel **12**(5): 607-15.

Ng, H. H., F. Robert, et al. (2003). "Targeted recruitment of Set1 histone methylase by elongating Pol II provides a localized mark and memory of recent transcriptional activity." Mol Cell **11**(3): 709-19.

Ng, S. S., K. L. Kavanagh, et al. (2007). "Crystal structures of histone demethylase JMJD2A reveal basis for substrate specificity." Nature **448**(7149): 87-91.

Nordlie, R. C., J. D. Foster, et al. (1999). "Regulation of glucose production by the liver." Annu Rev Nutr **19**: 379-406.

Okada, Y., G. Scott, et al. (2007). "Histone demethylase JHDM2A is critical for Tnp1 and Prm1 transcription and spermatogenesis." Nature **450**(7166): 119-23.

Pena, P. V., F. Davrazou, et al. (2006). "Molecular mechanism of histone H3K4me3 recognition by plant homeodomain of ING2." Nature **442**(7098): 100-3.

Pison, C. M., C. Chauvin, et al. (1998). "In vivo hypoxic exposure impairs metabolic adaptations to a 48 hour fast in rats." Eur Respir J **12**(3): 658-65.

Roth, S. Y., J. M. Denu, et al. (2001). "Histone acetyltransferases." Annu Rev Biochem **70**: 81-120.

Ruthenburg, A. J., C. D. Allis, et al. (2007). "Methylation of lysine 4 on histone H3: intricacy of writing and reading a single epigenetic mark." Mol Cell **25**(1): 15-30.

Santos-Rosa, H., R. Schneider, et al. (2002). "Active genes are tri-methylated at K4 of histone H3." Nature **419**(6905): 407-11.

Scacheri, P. C., S. Davis, et al. (2006). "Genome-wide analysis of menin binding provides insights into MEN1 tumorigenesis." PLoS Genet **2**(4): e51.

Schneider, J. and A. Shilatifard (2006). "Histone demethylation by hydroxylation: chemistry in action." ACS Chem Biol **1**(2): 75-81.

Schneider, J. E., J. Bose, et al. (2004). "Identification of cardiac malformations in mice lacking Ptdsr using a novel high-throughput magnetic resonance imaging technique." BMC Dev Biol **4**: 16.

Sen, G. L., D. E. Webster, et al. (2008). "Control of differentiation in a self-renewing mammalian tissue by the histone demethylase JMJD3." Genes Dev **22**(14): 1865-70.

She, P., M. Shiota, et al. (2000). "Phosphoenolpyruvate carboxykinase is necessary for the integration of hepatic energy metabolism." Mol Cell Biol **20**(17): 6508-17.

Shi, X., T. Hong, et al. (2006). "ING2 PHD domain links histone H3 lysine 4 methylation to active gene repression." Nature **442**(7098): 96-9.

Shi, Y., F. Lan, et al. (2004). "Histone demethylation mediated by the nuclear amine oxidase homolog LSD1." Cell **119**(7): 941-53.

Shi, Y. and J. R. Whetstine (2007). "Dynamic regulation of histone lysine methylation by demethylases." Mol Cell **25**(1): 1-14.

Sims, R. J., 3rd, S. Millhouse, et al. (2007). "Recognition of trimethylated histone H3 lysine 4 facilitates the recruitment of transcription postinitiation factors and pre-mRNA splicing." Mol Cell **28**(4): 665-76.

Skarnes, W. C., J. E. Moss, et al. (1995). "Capturing genes encoding membrane and secreted proteins important for mouse development." Proc Natl Acad Sci U S A **92**(14): 6592-6.

Smale, S. T. "Selective transcription in response to an inflammatory stimulus." Cell **140**(6): 833-44.

Smith, B. C. and J. M. Denu (2009). "Chemical mechanisms of histone lysine and arginine modifications." Biochim Biophys Acta **1789**(1): 45-57.

Stavropoulos, P., G. Blobel, et al. (2006). "Crystal structure and mechanism of human lysine-specific demethylase-1." Nat Struct Mol Biol **13**(7): 626-32.

Strahl, B. D. and C. D. Allis (2000). "The language of covalent histone modifications." Nature **403**(6765): 41-5.

Suganuma, T. and J. L. Workman (2008). "Crosstalk among Histone Modifications." Cell **135**(4): 604-7.

Takeuchi, T., Y. Watanabe, et al. (2006). "Roles of jumonji and jumonji family genes in chromatin regulation and development." Dev Dyn **235**(9): 2449-59.

Takeuchi, T., Y. Yamazaki, et al. (1995). "Gene trap capture of a novel mouse gene, jumonji, required for neural tube formation." Genes Dev **9**(10): 1211-22.

Tateishi, K., Y. Okada, et al. (2009). "Role of Jhdm2a in regulating metabolic gene expression and obesity resistance." Nature **458**(7239): 757-61.

Taverna, S. D., H. Li, et al. (2007). "How chromatin-binding modules interpret histone modifications: lessons from professional pocket pickers." Nat Struct Mol Biol **14**(11): 1025-40.

Testa, G., J. Schaft, et al. (2004). "A reliable lacZ expression reporter cassette for multipurpose, knockout-first alleles." Genesis **38**(3): 151-8.

Testa, G., Y. Zhang, et al. (2003). "Engineering the mouse genome with bacterial artificial chromosomes to create multipurpose alleles." Nat Biotechnol **21**(4): 443-7.

Trewick, S. C., P. J. McLaughlin, et al. (2005). "Methylation: lost in hydroxylation?" EMBO Rep **6**(4): 315-20.

Tsukada, Y., J. Fang, et al. (2006). "Histone demethylation by a family of JmjC domain-containing proteins." Nature **439**(7078): 811-6.

Tsukada, Y., T. Ishitani, et al. "KDM7 is a dual demethylase for histone H3 Lys 9 and Lys 27 and functions in brain development." Genes Dev **24**(5): 432-7.

Valk-Lingbeek, M. E., S. W. Bruggeman, et al. (2004). "Stem cells and cancer; the polycomb connection." Cell **118**(4): 409-18.

van Haaften, G., G. L. Dalgliesh, et al. (2009). "Somatic mutations of the histone H3K27 demethylase gene UTX in human cancer." Nat Genet **41**(5): 521-3.

Walter, W., D. Clynes, et al. (2008). "14-3-3 interaction with histone H3 involves a dual modification pattern of phosphoacetylation." Mol Cell Biol **28**(8): 2840-9.

Wang, G. G., L. Cai, et al. (2007). "NUP98-NSD1 links H3K36 methylation to Hox-A gene activation and leukaemogenesis." Nat Cell Biol **9**(7): 804-12.

Wang, J., S. Hevi, et al. (2009). "The lysine demethylase LSD1 (KDM1) is required for maintenance of global DNA methylation." Nat Genet **41**(1): 125-9.

Wang, N. D., M. J. Finegold, et al. (1995). "Impaired energy homeostasis in C/EBP alpha knockout mice." Science **269**(5227): 1108-12.

Whetstine, J. R., A. Nottke, et al. (2006). "Reversal of histone lysine trimethylation by the JMJD2 family of histone demethylases." Cell **125**(3): 467-81.

Yamane, K., K. Tateishi, et al. (2007). "PLU-1 is an H3K4 demethylase involved in transcriptional repression and breast cancer cell proliferation." Mol Cell **25**(6): 801-12.

Yamane, K., C. Toumazou, et al. (2006). "JHDM2A, a JmjC-containing H3K9 demethylase, facilitates transcription activation by androgen receptor." Cell **125**(3): 483-95.

Yang, X. J. and S. Gregoire (2005). "Class II histone deacetylases: from sequence to function, regulation, and clinical implication." Mol Cell Biol **25**(8): 2873-84.

Yap, K. L. and M. M. Zhou (2006). "Structure and function of protein modules in chromatin biology." Results Probl Cell Differ **41**: 1-23.

Zhang, Y., J. P. Muyrers, et al. (2000). "DNA cloning by homologous recombination in Escherichia coli." Nat Biotechnol **18**(12): 1314-7.

APPENDIX

Generation of *Jmjd3* conditional Knockout mouse

The full knockout does not allow us to address the role of Jmjd3 in inflammation in vivo because the mice are early lethal. To obtain viable mice with a selective lack of expression of Jmjd3 in cells of the innate immune system, we decided to generate conditional knockout mice.

Introduction

See the main text, Chapter 1.

Material and methods

Materials

Cell lines:

Name	Description	Source
EMFi	Inactivated mouse embryo fibroblast	C57BL/6
ES cell	Mouse embryonic stem cell	C57BL/6

Tissue culture reagents:

Plasticware: All standard tissue culture plasticware was obtained from Corning, Costar or Falcon.

Media, sera, supplements:

- DMEM (Gibco)
- Foetal Bovine Serum (Gibco)

Methods

Design of the *Jmjd3* targeting vector : The design and assembly of the targeting vector was based on Red/ET recombination ('recombineering') (Zhang, Muyrers et al. 2000) (Fig. A1). This technology uses phage-mediated homologous recombination in E.coli and one of its most relevant applications of this technology was the fluent engineering of bacterial artificial chromosomes (BACs) for the development of multipurpose alleles, whereby a concerted array of mutations and/or functional elements, two of which are flanked by FRT or loxP sites, are placed into a mouse locus in only one round of ES cell targeting (Testa, Zhang et al. 2003). Here we employed a variation of this technology, termed 'knock-out first', that combines the advantages of knock-out and conditional alleles in a single targeting effort, offering significant benefits in terms of economy, speed, and number of mouse lines required for the several purposes (Testa, Schaft et al. 2004). It is based on inserting a cassette (trap cassette) into an intron of an intact gene that produces a knock-out at the RNA processing level. FLPe and Cre recombinases systems are combined to allow, respectively, restoration of gene function through removal of the trap cassette, and conditional ablation of gene function through excision of an essential exon or set of exons.

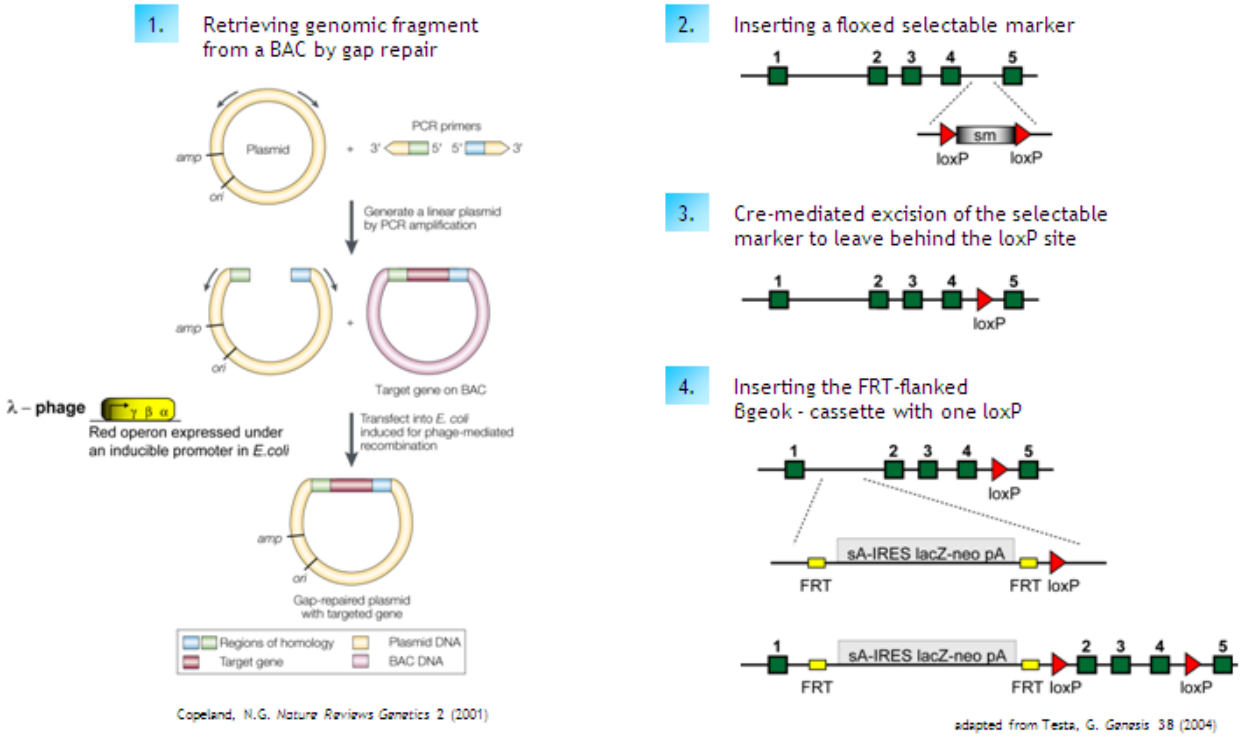

Figure A1. Generating the conditional knockout targeting vector by Red/ET recombination

The vector used for the generation of a conditional *Jmjd3* allele contains a splice acceptor (SA)-IRES-lacZ-neo-polyA, in which a bacterial promoter cloned in frame between the lacZ and the neomycin resistance gene enables selection in E. coli. The cassette is flanked by FRT sites, while two loxP sites surround essential or frame-shifting exons. Following homologous recombination, the baseline configuration of the allele generates a full knock-out allele at the RNA processing level. Following FLP-mediated recombination, gene function is restored, leaving a loxP-flanked (floxed) allele for Cre-mediated excision in the germline and/or in the various tissues of interest.

Production of fibroblast feeder layers: Since we used C57BL/6-derived embryonic stem (ES) cells for generating conditional *Jmjd3* knockout mouse and this type of ES cells are feeder-dependent cell line, we prepared EMFi cell stocks in which we obtained the vials of EF0 from stem cell facility in the campus and passage them on two 150mm dish. After plate

becoming confluent, which takes 3-4 days after seeding, each dish was expanded 1:5 in to 150mm plates. The Emfi's were inactivated using mitomycin C (Mmc) for 3 hrs and tripsinized and harvested. From each 150mm plate, 3 vials of EMFi were prepared for freezing. Each frozen vial were used later for growing ES cells on one 100 mm plate.

ES cell line: C57BL/6-derived ES were maintained in high glucose DMEM supplemented with 20% Foetal Bovine Serum, 1% glutamine, 1% NEAA, 0.1% β-mercaptoethanol, HEPES, LIF.

Eloctroporation of linearized *jmjd3* targeting vector in to ES cells: The *Jmjd3* targeting vector was linearized by I-SceI restriction enzyme (5U enzyme per each µg of plasmidDNA).

Plasmid	**120 µg**
I-SceI	120 µl (600 unit)
10X buffer	130 µl
100X BSA	13 µl
ddH2O	Up to 1300 µl
Total vol.	1300 µl

The resulting vector was electroporated into C57BL6/J-derived embryonic stem (ES) cells and these were selected for resistance to G418 for 8-10 days .

Identification of ES clones carrying a *Jmjd3* targeted allele by southern blotting:

After selection period, resistant ES cell clones were picked and screened by southern blot analysis using the strategy depicted in Fig. A2 to identify homologous recombinants. Two different southern blot probes; one at the 5' site and another at the 3' site, were designed for finding the targeted clones. For generating 5' probe, part of the 5' site of *jmjd3* was cloned in bluescript plasmid and then by using EcoRI and HindIII restriction enzymes, a fragment with 555 bp length was cut and used as a probe. For 3' site, two different probes were generated by PCR.

Probe name	Forward primer	Reverse primer	Product size (bp)
PbN33	CCA AGT ACA GCA GCC CTC AGA C	GAC CTT CAT GTA TAG CTG CAC GG	681
PbN34	TGG AAC GAG GTG AAG AAC GTC	CTC ATC GAG ACG TGC TGG C	989

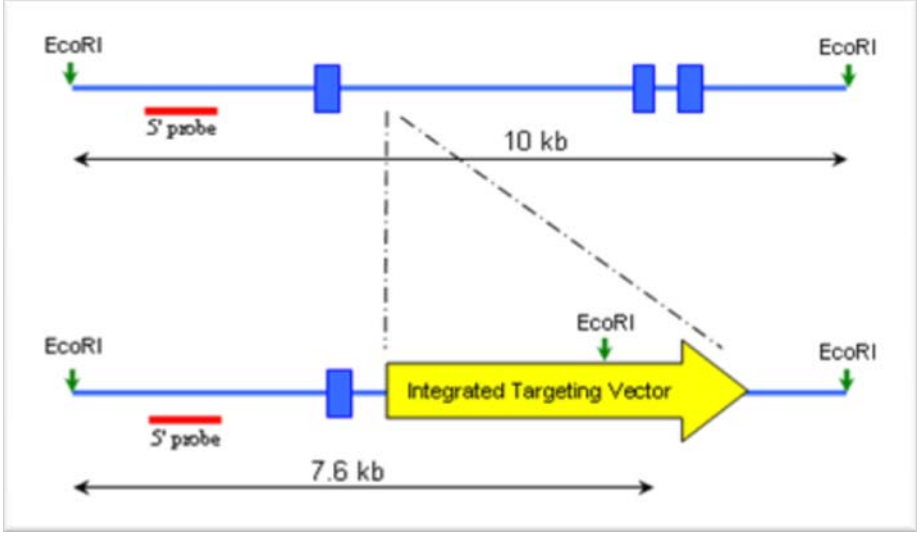

Figure A2. Southern blot strategy to distinguish *Jmjd3* wild type (upper line) and targeted (lower line) alleles.

Confirmation of the only once integration of the construct in the genome:

There is a chance of more than one integration of the targeting vector in the genome during the electroporation. To confirm that we had only one integration event not more in the mouse genome, we used southern blotting with the probe designed in the Neo-resistance gene.
In case of more than one integration, more than one band could be seen in the southern blot with different size.

Confirming the presence of the LoxP site in the positive clones:

Three exons of *Jmjd3* are located between two LoxP sites. During the homologous recombination event between the 5' and 3' homology arms, there is a chance to have a homologous recombination event between the 5' homology arm and the exons located between two LoxP sites instead of the 3' homology arm. In this case, we would lose the second LoxP site in the targeted allele. To confirm the presence of the second LoxP site which is close to the 3' part, we designed primers before and after the second LoxP site (Figure A3).

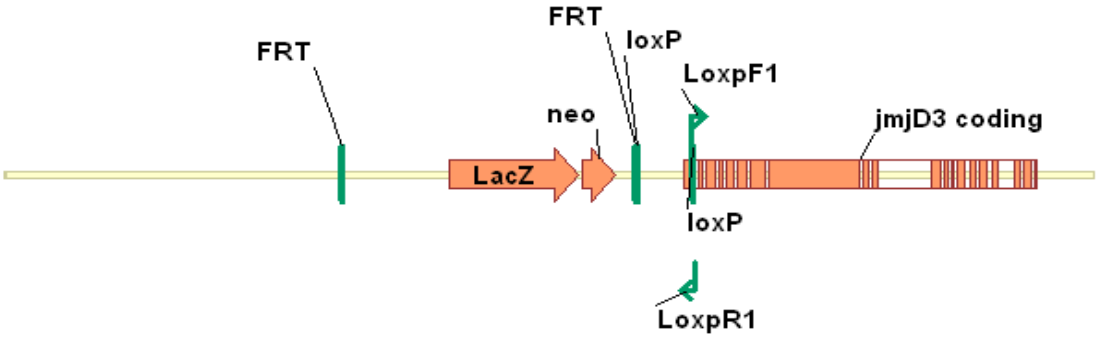

Figure A3. Schematic representation of LoxP-PCR strategy.

Tat-Cre treatment of the targeted ES cell clones

For Tat-Cre transduction test, the targeted ES cells were plated on a 10-cm^2 dish culture plate in normal culture medium for 24h. The ES cells were trypsinized and counted. 200,000-targeted ES cells were then plated on a 6-well tissue culture plate. After 6 h , the cells were washed 5X with a 1:1 mixture of PBS and DMEM to remove any protein in medium. The ES cells were then incubated for 16-18 h in a PBS:DMEM (1:1) medium containing 5µM of Tat-Cre protein. Cells were washed once with PBS after transduction and furthure cultivated for 1-2 days in normal medium before being trypsinized and passaged. DNA was prepared from the treated ES cells and routine PCR was done to confirm: i) co-integration of the selectable cassette and the second loxP site on the same allele, and ii) the function of the two loxP sites. Cre excision was detected by PCR with primers spanning the floxed exons.

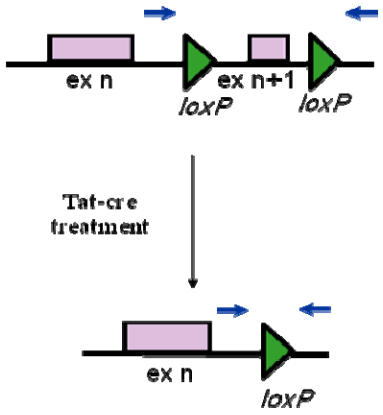

Figure A4. Strategy used for Tat-Cre experiment.

PCR product size for the untreated ES cells is 1.5 kb and the expected product size after treatment is 182 bp. The sequence of the primers and the PCR program is mentioned below:

Primers:

Forward (PolyA-f) 5'- TCT TAT CAT GTC TGG ATC CGG – 3'

Reverse (LoxpR1) 5' – GGA AGA GCA GAT GAG ACT GG - 3'

PCR program:

98°C	30 sec.	
98°C	10 sec.	40X
63.5°C	30 sec.	
72°C	15 sec.	
72°C	5 min.	

Karyotyping

For chromosome spreads 0.25×10^{6} ES cells were plated on a 6-well tissue culture plate. After 24h the cells were incubated with colcemid (Gibco) at a final concentration of 0.1 μg/ml for 1h at 37°C. The cells were then trypsinized, centrifuged, and resuspended in 0.5 ml remaining medium by gently flicking the tube. Ten milliliter of hypotonic solution (0.075 M KCl in H_2O) was added dropwise while gently flicking the tube and the resulting suspension was incubated for 25 min at 37°C. Ten drops of fixative (methanol:acetic acid, 3:1) was added to the tube. After centrifugation for 5 min at 1200 rpm the pellet was resuspended in 0.5 ml hypotonic solution by gently flicking. Then 5 ml of fixative (methanol:acetic acid, 3:1) was added dropwise while gently vortexing. Fixed cells were then centrifuged (5 min, 1200 rpm), again resuspended in 3 ml of fixative while gently flicking. 60μl of the fixed cells were dropped on the wet slide keeping on the top of 50°C water-bath.

The dried slides were stained by DAPI (5000X) in 2X SSC solution for 5 min. The stained slides were dried in a dark place and mounted with DABCO solution (0.233gr DABCO, 800µl H_2O, 200µl 1M Tris-HCl and 9ml Glycerol). The prepared slides were analyzed under microscope.

RESULT

Production of *Jmjd3* targeted ES cell clones:

Of 765 resistant ES cell clones, 295 were screened by southern blot analysis for presence of a 7.6-kb EcoRI fragment for the 5' site using the strategy depicted in Fig. A2. Twenty four correctly targeted ES clones were identified (Fig. A5).

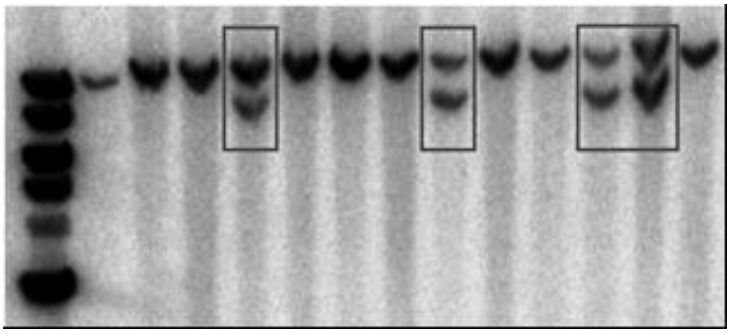

Figure A5. Southern blot analysis of infected ES cells with *jmjd3* targeting vector. The 10 kilobase (kb) fragment (upper band) reperesents the endogenous wild-type *jmjd3* allele and the 7.6 kb band (lower band) the targeted *jmjd3* allele.

To ascertain that there was no breakage in the whole targeted construct and the 3' part of the construct was also present in the targeted allele, 3' southern blot was done for the positive clones using the strategy mentioned before (Fig. A6).

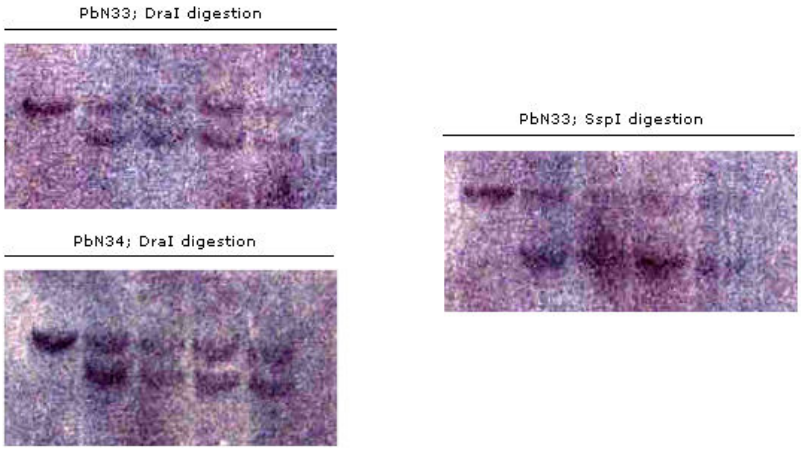

Figure A6. Southern blot analysis for 3' site. PbN33 and PbN34 were used as probe. 13.5-kb wild-type (WT) and 10.4-kb targeted (tg) alleles in DraI digestion and 16-kbp wild-type (WT) and 11.4-kbp tg alleles in SspI digestion are indicated.

Confirmation of the only once integration of the construct in the genome:

As we saw only one band in Southern blot filter hybridized with Neo Probe, only one integration of the *Jmjd3* targeting vector in the mouse genome was confirmed (Fig. A7).

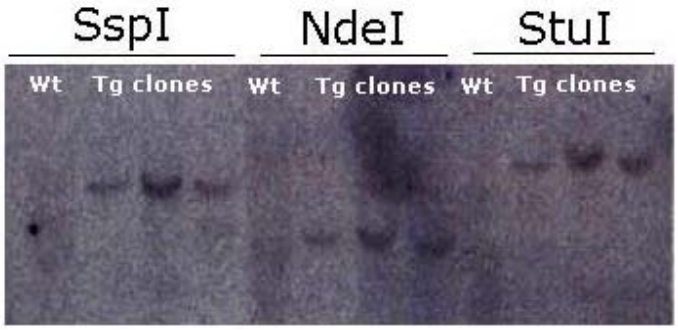

Figure A7. Southern blot analysis with Neo probe.

Confirming the presence of the LoxP site in the positive clones:

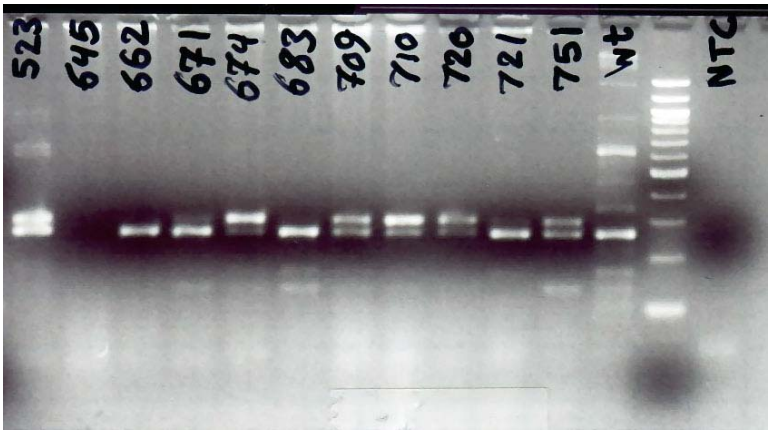

Figure A8. Representative photo showing PCR analysis of the targeted clones. The PCR bands of wild-type allele(264 bp) and targeted allele (298 bp) are indicated.

Tat-Cre treatment of the targeted ES cell clones

Targeted ES cell clones were treated with the cell permeable TAT-Cre fusion protein to confirm: i) co-integration of the selectable cassette and the second loxP site on the same allele, and ii) the function of the two loxP sites. Cre excision was detected by PCR with primers spanning the floxed exons (Fig. A9).

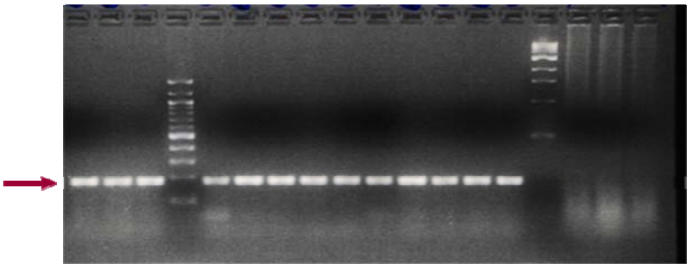

Figure A9. PCR amplicon resulting from Cre-mediated excision of the floxed exons.

Karyotyping:

Karyotype analysis of some of the targeted ES cell clones showed no chromosomal loss or abnormality (Fig. A10). Clones selected for injection in blastocyst.

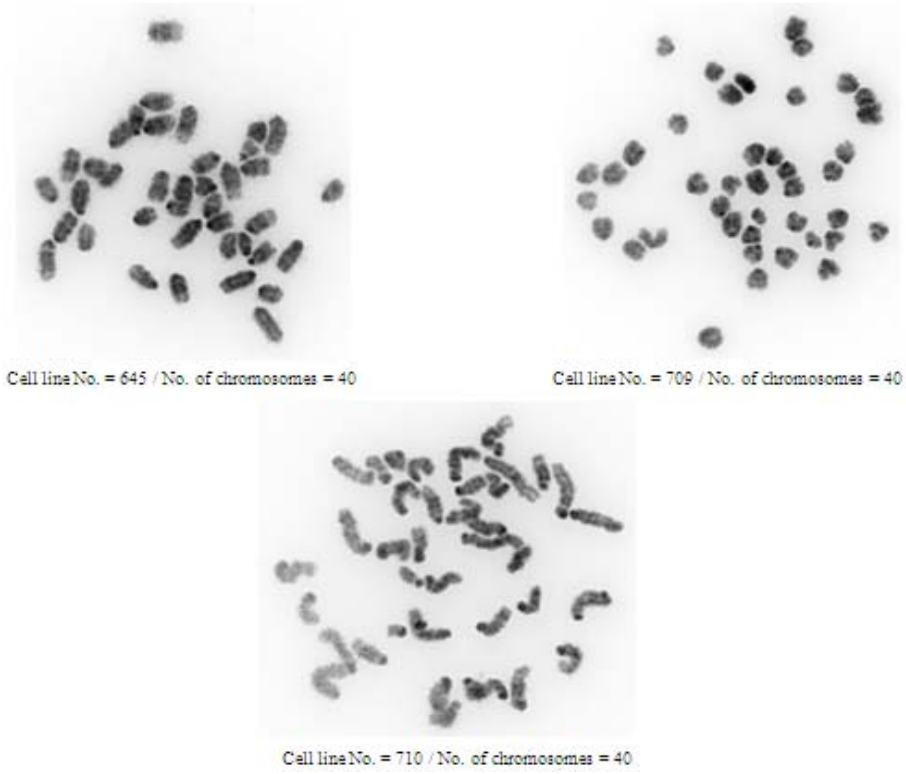

Figure A10. Karyotype analysis of targeted ES cell clones

Up to now, we got some chimera without getting any germline-transmitted mice. Since the gene targeting strategy which we used is a knockout first strategy and in the targeted clones, basically one copy of the *Jmjd3* is off. We suppose probably sperm with just one copy of the gene cannot function normally.

To overcome this problem, we tried to remove the cassette by Flp recombinase treatment and inject the ES clones in to the blastocyst. Already the clones have been injected in to the normal C57BL6/J pseudo pregnant mice. This part of project is still ongoing.